

**Spin-glass phase transitions and minimum energy of the random feedback vertex set problem**Shao-Meng Qin,<sup>1,2,\*</sup> Ying Zeng,<sup>3</sup> and Hai-Jun Zhou<sup>1,4,†</sup><sup>1</sup>*Institute of Theoretical Physics, Chinese Academy of Sciences, Zhong-Guan-Cun East Road 55, Beijing 100190, China*<sup>2</sup>*College of Science, Civil Aviation University of China, Tianjin 300300, China*<sup>3</sup>*Beijing National Laboratory for Condensed Matter Physics and Key Laboratory of Soft Matter Physics, Institute of Physics, Chinese Academy of Sciences, Beijing 100190, China*<sup>4</sup>*School of Physical Sciences, University of Chinese Academy of Sciences, Beijing 100049, China*

(Received 15 February 2016; revised manuscript received 27 July 2016; published 29 August 2016)

A feedback vertex set (FVS) of an undirected graph contains vertices from every cycle of this graph. Constructing a FVS of sufficiently small cardinality is very difficult in the worst cases, but for random graphs this problem can be efficiently solved by converting it into an appropriate spin-glass model [H.-J. Zhou, *Eur. Phys. J. B* **86**, 455 (2013)]. In the present work we study the spin-glass phase transitions and the minimum energy density of the random FVS problem by the first-step replica-symmetry-breaking (1RSB) mean-field theory. For both regular random graphs and Erdős-Rényi graphs, we determine the inverse temperature  $\beta_l$  at which the replica-symmetric mean-field theory loses its local stability, the inverse temperature  $\beta_d$  of the dynamical (clustering) phase transition, and the inverse temperature  $\beta_s$  of the static (condensation) phase transition. These critical inverse temperatures all change with the mean vertex degree in a nonmonotonic way, and  $\beta_d$  is distinct from  $\beta_s$  for regular random graphs of vertex degrees  $K > 60$ , while  $\beta_d$  are identical to  $\beta_s$  for Erdős-Rényi graphs at least up to mean vertex degree  $c = 512$ . We then derive the zero-temperature limit of the 1RSB theory and use it to compute the minimum FVS cardinality.

DOI: [10.1103/PhysRevE.94.022146](https://doi.org/10.1103/PhysRevE.94.022146)**I. INTRODUCTION**

A undirected graph is formed by a set of vertices and a set of undirected edges between the vertices. A cycle (or a loop) of such a graph is a closed path connected by a set of different edges. A feedback vertex set (FVS) is a subset of vertices intersecting with every cycle of this graph [1]. If all the vertices in a FVS are deleted from the graph, then there will be no cycle in the remaining subgraph. The FVS problem aims at constructing a FVS of cardinality (size) not exceeding a certain prespecified value or proving the nonexistence of such a FVS [1,2]. This problem has wide practical applications, such as combinatorial circuit design [1] and deadlock recovery in operating systems [3], network dynamics analysis [4,5], epidemic spreading [6], and network targeted attack and optimal percolation [7,8].

The FVS problem is a combinatorial optimization problem in the nondeterministic polynomial-complete (NP-complete) complexity class [9]. It is generally believed (yet not rigorously proven) to be unsolvable by a complete algorithm in time bounded by a polynomial function of the number of vertices or edges in the graph, except for some special instances on which this problem can be solved by polynomial algorithms, like cubic graphs [10], permutation graphs [11], and interval graphs [12]. So far, the most efficient complete algorithm constructs a FVS of global minimum cardinality in time  $\propto 1.7548^N$  by solving the equivalent maximum induced forest problem [13]. Many heuristic algorithms have been developed to solve the FVS problem approximately. These algorithms are incomplete as they may fail for some input graph instances, but they have the merit of reaching a FVS solution very quickly. One famous heuristic algorithm is the

FEEDBACK algorithm of Bafna and coauthors [14], which is guaranteed to return a FVS solution of cardinality at most 2 times the minimum value for any input graph. In a more recent paper, two of the present authors demonstrated that a heuristic algorithm based on the idea of simulated annealing extensively outperforms FEEDBACK on random graphs and finite-dimensional lattices [15]. The FVS problem has also been treated by statistical physics methods and the associated belief propagation-guided decimation (BPD) algorithm [16]. This physics-inspired message-passing algorithm outperforms simulated annealing to some extent and constructs a FVS of cardinality being very close to the global minimum value.

The spin-glass model in Ref. [16] implements the global cycle constraints as a set of local edge constraints, with each vertex having only three essentially different states. This spin-glass model was then studied by mean-field theory at the level of replica symmetry (RS). At low temperatures (equivalently high inverse temperatures  $\beta$ ), the RS iterative equations could not reach a self-consistent solution [16], which indicates that the RS theory is valid only at sufficiently high temperatures and that the low-temperature property of the FVS spin-glass model is very complex. In the present paper, we continue to study this spin-glass model at finite temperatures and at the zero temperature limit using the first-step replica-symmetry-breaking (1RSB) mean-field theory [17–19]. We mainly work on the ensemble of regular random (RR) graphs and in some cases also consider the ensemble of Erdős-Rényi (ER) random graphs. The degree of a vertex is defined as the number of edges attached to this vertex. Each vertex in a RR graph has the same degree  $K$ , but the edges in the graph are connected completely at random. On the other hand, an ER graph is created by setting up  $M = (c/2)N$  edges completely at random between  $N$  vertices, where  $c$  is the mean vertex degree. When  $N$  is sufficiently large, the degree of a randomly chosen vertex follows the Poisson distribution with mean value  $c$  [20].

\*qsminside@163.com

†Corresponding author: zhouhj@itp.ac.cn

After reviewing the spin-glass model and the RS mean-field theory in Sec. II, we analyze in Sec. III the local stability of the RS theory analytically for RR graphs and numerically for ER graphs and then study the dynamical (clustering) and static (condensation) spin-glass transitions in Sec. IV. We determine the critical inverse temperature  $\beta_l$  for the local stability of the RS theory, the inverse temperature  $\beta_d$  of the dynamical transition, and the inverse temperature  $\beta_s$  of the static transition. We find that these critical inverse temperatures change with the (mean) vertex degree in a nonmonotonic way. The inverse temperature  $\beta_l$  coincides with  $\beta_d$  when  $K$  or  $c$  is relatively small. But  $\beta_l$  exceeds  $\beta_d$  when  $K > 35$  for RR graphs or  $c > 100$  for ER graphs and  $\beta_l$  may even exceeds  $\beta_s$ , suggesting that the RS mean-field theory can still be locally stable even when the system is deep in the spin-glass phase. For the ER graph ensemble we find that  $\beta_d$  is indistinguishable from  $\beta_s$  for all the mean vertex degrees explored (up to  $c = 512$ ), but for the RR graph ensemble of  $K > 60$  we find that  $\beta_s > \beta_d$ . The existence of two distinct spin-glass phases for dense RR graphs is not yet fully understood and needs to be further investigated.

In Sec. V we derive the  $\beta \rightarrow \infty$  limit of the 1RSB mean-field theory and use the resulting survey propagation (SP) equation to compute the ensemble-averaged minimum FVS cardinality. Our zero-temperature 1RSB results improve over the RS mean-field results, and they are in agreement with some known rigorous mathematical results [21,22], the mean-field results of another closely related work [6], and the algorithmic results of Refs. [15,16]. We point out that the zero-temperature SP equation can be exploited by message-passing algorithms to achieve even better FVS solutions for single graph instances than the BPD algorithm.

Cycles are nonlocal properties of random graphs, and the cycle constraints in the undirected FVS problem are therefore global in nature. Phase transitions in globally constrained spin-glass models and combinatorial optimization problems are usually very hard to investigate. We believe the results reported in this paper will also shed light on the energy landscape properties of other globally constrained problems.

## II. MODEL AND REPLICA-SYMMETRIC THEORY

We consider an undirected simple graph  $\mathcal{G}$  formed by  $N$  vertices and  $M$  edges. There is no self-edge from a vertex to itself, and there is at most one edge between any pair of vertices. For each vertex  $i \in \{1, 2, \dots, N\}$  we denote by  $\partial i$  the set of vertices that are connected to  $i$  through an edge. The degree  $d_i$  of vertex  $i$  is then the cardinality of  $\partial i$  ( $d_i \equiv |\partial i|$ ).

### A. Local constraints and partition function

We assign a state  $A_i$  to each vertex  $i$  of graph  $\mathcal{G}$ .  $A_i$  can take  $(d_i + 2)$  possible non-negative integer values from the union set  $\{0, i\} \cup \partial i$ . If  $A_i = 0$ , then vertex  $i$  is regarded as being empty, and otherwise it is occupied. In the latter case, if  $A_i = i$ , then we say  $i$  is a root vertex, and otherwise  $A_i = j \in \partial i$  and we say  $j$  is the parent vertex of  $i$ .

To represent the global cycle constraints in a distributed way, we define for each edge  $(i, j)$  between vertices  $i$  and  $j$  a

counting number  $C_{(i,j)}$  as [16]

$$\begin{aligned} C_{(i,j)}(A_i, A_j) &\equiv \delta_{A_i}^0 \delta_{A_j}^0 \\ &+ \delta_{A_i}^0 (1 - \delta_{A_j}^0 - \delta_{A_j}^i) + \delta_{A_j}^0 (1 - \delta_{A_i}^0 - \delta_{A_i}^j) \\ &+ \delta_{A_i}^j (1 - \delta_{A_j}^0 - \delta_{A_j}^i) + \delta_{A_j}^i (1 - \delta_{A_i}^0 - \delta_{A_i}^j), \end{aligned} \quad (1)$$

where  $\delta_b^a = 1$  if  $a = b$  and  $\delta_b^a = 0$  if  $a \neq b$ . This counting number is either 0 or 1. We say that edge  $(i, j)$  is satisfied if and only if  $C_{ij}(A_i, A_j) = 1$ ; otherwise this edge is regarded as unsatisfied. A microscopic configuration  $\underline{A} \equiv (A_1, A_2, \dots, A_N)$  is called a legal configuration if and only if it satisfies all the  $M$  edges. A legal configuration  $\underline{A}$  has an important graphical property: Each connected component of the subgraph induced by all the occupied vertices of  $\underline{A}$  is either a tree (which has  $n \geq 1$  vertices and  $n - 1$  edges) or a so-called cycle-tree (which contains a single cycle and has  $n \geq 2$  vertices and  $n$  edges) [16].

Given a legal configuration  $\underline{A}$  of graph  $\mathcal{G}$ , we can easily construct a feedback vertex set  $\Gamma$  as follows: (1) Add all the empty vertices of  $\underline{A}$  to  $\Gamma$ , and (2) if the subgraph induced by the occupied vertices of  $\underline{A}$  has one or more cycle-tree components, then for each cycle-tree component we add a randomly chosen vertex on the unique cycle to  $\Gamma$  to break this cycle [16]. On the other hand, given a feedback vertex set  $\Gamma$ , we can easily construct many legal configurations  $\underline{A}$  as follows: (1) Assign all the vertices  $i \in \Gamma$  the empty state  $A_i = 0$ , and (2) for each tree component (say,  $\tau$ ) of the subgraph induced by all the vertices outside  $\Gamma$ , randomly choose one vertex  $j \in \tau$  as the root ( $A_j = j$ ) and then determine the states of all the other vertices in  $\tau$  recursively: A nearest neighbor  $k$  of  $j$  has state  $A_k = j$  and a nearest neighbor  $l \neq j$  of  $k$  has state  $A_l = k$ , and so on.

We define the energy of a microscopic configuration  $\underline{A}$  as

$$E(\underline{A}) = \sum_{i=1}^N \delta_{A_i}^0, \quad (2)$$

which just counts the total number of empty vertices. Because of the mapping between legal configurations and feedback vertex sets, the energy function  $E(\underline{A})$  under the edge constraints (1) serves as a very good proxy to the energy landscape of the undirected FVS problem (see also Sec. II C). The minimum value of  $E(\underline{A})$  over all legal configurations is referred to as the ground-state energy and is denoted as  $E_0$  (and the ground-state energy density is  $e_0 \equiv E_0/N$ ). The corresponding configurations are the ground-state configurations and the number of all ground-state configurations is denoted as  $\Omega_0$ . Due to the effect of cycle-trees the ground-state energy  $E_0$  might be slightly lower than the cardinality of a minimum FVS, but the difference is negligible for  $N$  sufficiently large [16].

The partition function of our spin-glass model is

$$Z(\beta) = \sum_{\underline{A}} \exp[-\beta E(\underline{A})] \prod_{(i,j) \in \mathcal{G}} C_{(i,j)}(A_i, A_j), \quad (3)$$

where  $\beta$  is the inverse temperature. Notice that if a configuration is not legal, it has no contribution to  $Z(\beta)$ , therefore  $Z(\beta)$  is the sum of the statistical weights  $e^{-\beta E(\underline{A})}$  of all the legal configurations  $\underline{A}$ . The equilibrium probability of observing a

legal configuration  $\underline{A}$  is then

$$\mu(\underline{A}) = \frac{1}{Z(\beta)} \exp[-\beta E(\underline{A})] \prod_{(i,j) \in \mathcal{G}} C_{(i,j)}(A_i, A_j). \quad (4)$$

The total free energy of the system is related to the partition function through

$$F(\beta) = -\frac{1}{\beta} \ln Z(\beta). \quad (5)$$

The free energy has the limiting expression of  $F = E_0 - \frac{1}{\beta} \ln \Omega_0$  as  $\beta$  approaches infinity.

### B. Belief-propagation equation

The RS mean-field theory assumes that all the equilibrium configurations of the spin-glass model (3) form a single macroscopic state [19]. The states of two or more distantly separated vertices are then regarded as uncorrelated and their joint distribution is expressed as the product of individual vertices' marginal distributions. Let us denote by  $q_i^{A_i}$  the marginal probability of vertex  $i$ 's state being  $A_i$ . The state  $A_i$  is strongly affected by its nearest neighbors, and the states of the vertices in  $\partial i$  are also strongly correlated since all of them interact with  $i$ . Due to the local treelike structure of random graphs, if vertex  $i$  is removed, then the vertices in set  $\partial i$  will become distantly separated and their states may then be assumed as uncorrelated. For two vertices  $i$  and  $j$  connected by an edge  $(i, j)$ , let us denote by  $q_{j \rightarrow i}^{A_j}$  the marginal probability of  $j$  being in state  $A_j$  in the absence of  $i$  (such a probability is referred to as a cavity probability in the literature).

After considering the interactions of  $i$  with all the vertices in  $\partial i$ , the RS theory then predicts that [16]

$$q_i^0 = \frac{e^{-\beta}}{z_i}, \quad (6a)$$

$$q_i^i = \frac{1}{z_i} \prod_{j \in \partial i} [q_{j \rightarrow i}^0 + q_{j \rightarrow i}^j], \quad (6b)$$

$$q_i^j = \frac{1}{z_i} (1 - q_{j \rightarrow i}^0) \prod_{k \in \partial i \setminus j} [q_{k \rightarrow i}^0 + q_{k \rightarrow i}^k], \quad (j \in \partial i), \quad (6c)$$

where  $\partial i \setminus j$  means the set obtained by deleting vertex  $j$  from the set  $\partial i$ , and the normalization factor  $z_i$  is

$$z_i \equiv e^{-\beta} + \left[ 1 + \sum_{k \in \partial i} \frac{1 - q_{k \rightarrow i}^0}{q_{k \rightarrow i}^0 + q_{k \rightarrow i}^k} \right] \prod_{j \in \partial i} [q_{j \rightarrow i}^0 + q_{j \rightarrow i}^j]. \quad (7)$$

Similarly, the probabilities  $q_{i \rightarrow j}^{A_i}$  and  $q_{j \rightarrow i}^{A_j}$  on all the edges  $(i, j)$  can be self-consistently determined by a set of belief-propagation (BP) equations [16]:

$$q_{i \rightarrow j}^0 = \frac{e^{-\beta}}{z_{i \rightarrow j}}, \quad (8a)$$

$$q_{i \rightarrow j}^i = \frac{1}{z_{i \rightarrow j}} \prod_{k \in \partial i \setminus j} [q_{k \rightarrow i}^0 + q_{k \rightarrow i}^k], \quad (8b)$$

$$q_{i \rightarrow j}^l = \frac{1}{z_{i \rightarrow j}} (1 - q_{l \rightarrow i}^0) \prod_{k \in \partial i \setminus j, l} [q_{k \rightarrow i}^0 + q_{k \rightarrow i}^k], \quad (8c)$$

where  $l \in \partial i \setminus j$  in Eq. (8c) and  $\partial i \setminus j, l$  means the set obtained by deleting vertices  $j$  and  $l$  from  $\partial i$ , and the normalization factor  $z_{i \rightarrow j}$  is

$$z_{i \rightarrow j} \equiv e^{-\beta} + \left[ 1 + \sum_{k \in \partial i \setminus j} \frac{1 - q_{k \rightarrow i}^0}{q_{k \rightarrow i}^0 + q_{k \rightarrow i}^k} \right] \prod_{l \in \partial i \setminus j} [q_{l \rightarrow i}^0 + q_{l \rightarrow i}^l]. \quad (9)$$

In our later discussions, Eq. (8) will be abbreviated as  $q_{i \rightarrow j} = b(\{q_{k \rightarrow i}\})$ .

At a fixed point of the BP equation (8), we can evaluate the total free energy (5) as the sum of contributions from all vertices minus that from all edges [16]:

$$F = \sum_{i=1}^N f_i - \sum_{(i,j) \in \mathcal{G}} f_{ij}. \quad (10)$$

The free-energy contributions  $f_i$  and  $f_{ij}$  of a vertex  $i$  and an edge  $(i, j)$  are computed through

$$f_i = -\frac{1}{\beta} \ln[z_i], \quad (11)$$

$$f_{ij} = -\frac{1}{\beta} \ln[q_{i \rightarrow j}^0 q_{j \rightarrow i}^0 + (1 - q_{i \rightarrow j}^0)(q_{j \rightarrow i}^0 + q_{j \rightarrow i}^j) + (1 - q_{j \rightarrow i}^0)(q_{i \rightarrow j}^0 + q_{i \rightarrow j}^i)]. \quad (12)$$

The expression for the mean total energy  $\langle E \rangle$  is

$$\langle E \rangle = \sum_{i=1}^N q_i^0 = e^{-\beta} \sum_{i=1}^N \frac{1}{z_i}. \quad (13)$$

The RS mean-field equations (6), (8), and (10) are applicable to single graph instances. We can also use these equations to obtain the ensemble-averaged results. At the thermodynamic limit of  $N \rightarrow \infty$ , a random graph is characterized by its degree distribution  $P(d)$ , which is the probability of a randomly chosen vertex having  $d$  nearest neighbors. As there is no degree correlation in a random graph, the probability  $Q(d)$  that the degree of the vertex at the end of a randomly chosen edge being  $d$  is related to  $P(d)$  through

$$Q(d) = \frac{d P(d)}{\sum_{d' \geq 1} d' P(d')} \quad (d \geq 1). \quad (14)$$

In the literature  $Q(d)$  is often referred to as the excess degree distribution. For the RR ensemble  $P(d) = Q(d) = \delta_d^K$ ; for the ER ensemble  $P(d) = \frac{e^{-c} c^d}{d!}$  and  $Q(d) = \frac{e^{-c} c^{d-1}}{(d-1)!}$  (both are Poisson distributions).

Let us denote by  $\mathcal{P}[q_{i \rightarrow j}]$  the probability functional of the cavity distributions  $q_{i \rightarrow j}$ , which gives the probability that a randomly picked edge  $(i, j)$  of the graph has the cavity probability distribution  $q_{i \rightarrow j}$ . This probability functional is governed by the following self-consistent equation:

$$\mathcal{P}[q] = \sum_{d=1}^{\infty} Q(d) \int \prod_{j=1}^{d-1} \mathcal{D}q_j \mathcal{P}[q_j] \delta[q - b(\{q_j\})], \quad (15)$$

where the Dirac  $\delta$  functional  $\delta[q - b(\{q_j\})]$  ensures that the output cavity distribution  $q$  and the set of input cavity distributions  $\{q_j\}$  are related by the BP equation (8).

For the RR graph ensemble, if we assume that the probability functional  $\mathcal{P}[q]$  is a Dirac delta functional, then the RS mean-field theory can be further simplified (see Appendix A). At the limit of degree  $K \rightarrow \infty$ , this simplified theory predicts the ground-state energy density to be  $e_0 \approx 1 - \frac{2 \ln K}{K}$ , which agrees with the rigorous results of Ref. [23].

### C. Some additional remarks

The described model (3) is essentially a three-state spin glass with each vertex  $i$  being empty ( $A_i = 0$ ), being a root ( $A_i = i$ ), or being a child ( $A_i \in \partial i$ ), and we need only to update the probabilities  $q_{i \rightarrow j}^0$  and  $q_{i \rightarrow j}^i$  through Eq. (8). Because of this convenience and the local nature of the edge constraints, the associated BPD algorithm is very efficient in solving the FVS problem and also the closely related network optimal attack problem for single graph instances [7,16].

On the theoretical side, as mentioned in Sec. II A, the model does not achieve a one-to-one mapping between legal configurations  $\underline{A}$  and FVS solutions. The model allows a connected component of occupied vertices to be a cycle-tree. This will cause a tiny change to the energy, since one vertex from each cycle-tree has to be deleted to bring it back to a tree. For sparse random graphs, after very few finite-length cycles are cut, the shortest cycle length in the remaining graph is of order  $\ln N$ , so the total number of cycle-trees will at most be of order  $N / \ln N$  and the energy density change will at most be of order  $1 / \ln N$ . So even in these worst cases the energetic effect of cycle-trees can be safely neglected when  $N$  is sufficiently large.

For each tree component formed by  $n$  occupied vertices there are  $n$  different ways of choosing the root vertex. Therefore, each forest of occupied vertices is associated with an entropic weight  $\prod_m n_m$ , where  $n_m$  is the size of the  $m$ th tree component in this forest [16]. But in the case of sparse random graphs this spurious entropic effect will not cause an extensive ground-state entropy. The simplest argument goes as follows: Since the length of shortest cycles in the giant connected component of the graph is of order  $\ln N$ , each tree component of the ground-state forest must contain at least  $O(\ln N)$  vertices and the total number of such trees will at most be of order  $N / \ln N$ ; consequently, the ground-state entropy will at most be of order  $\frac{N}{\ln N} \ln \ln N$  which is not extensive. If there are only a few minimum FVS solutions for the random graph, then the ground-state entropy density of model (3) will also approach zero (for  $N \rightarrow \infty$ ).

It is easy to map the FVS problem into a more conventional spin-glass model by defining on each vertex  $i$  a height state  $0 \leq h_i \leq D$  and then requiring that if  $h_i > 0$  then vertex  $i$  should have no neighbor of the same height and should have at most one neighbor  $j$  with height  $h_j > h_i$  (see, e.g., the last section of Ref. [16] and Refs. [6,24]). If the height limit  $D$  is set to be equal to  $N$ , then this latter model achieves a faithful representation of the FVS problem, but the computational cost is extremely huge. In numerical and theoretical computations [6,8], the maximum height  $D$  is always set to be much smaller than  $N$  and  $\lim_{N \rightarrow \infty} D/N = 0$ . As a consequence, the lengths of the typical cycles are all greatly exceeding the height limit  $D$  and the cycle constraints become completely irrelevant for the model. In contrast, the spin-glass model (3) does not introduce

any external height limit and all its constraints are directly related to cycles. We therefore believe that model (3) is a better model for the FVS problem on the conceptual level, in addition to its practical advantage.

## III. LOCAL STABILITY OF REPLICA-SYMMETRIC THEORY

Before treating the spin-glass model (3) by the 1RSB mean-field theory, let us first check the local stability of the RS theory. Assume that a BP fixed-point solution, say,  $\{\tilde{q}_{i \rightarrow j}, \tilde{q}_{j \rightarrow i} : (i, j) \in \mathcal{G}\}$ , has been reached. We perform a perturbation to this fixed point,

$$q_{i \rightarrow j}^0 = \tilde{q}_{i \rightarrow j}^0 + \epsilon_{i \rightarrow j}^0, \quad q_{i \rightarrow j}^i = \tilde{q}_{i \rightarrow j}^i + \epsilon_{i \rightarrow j}^i, \quad (16)$$

with  $\epsilon_{i \rightarrow j}^0, \epsilon_{i \rightarrow j}^i$  being sufficiently small. If the amplitudes of all these quantities  $\epsilon_{i \rightarrow j}^0$  and  $\epsilon_{i \rightarrow j}^i$  shrink during the iteration of Eqs. (8a) and (8b),  $q_{i \rightarrow j}^0$  and  $q_{i \rightarrow j}^i$  will relax back to  $\tilde{q}_{i \rightarrow j}^0$  and  $\tilde{q}_{i \rightarrow j}^i$ . We then say that the BP fixed point is locally stable; otherwise, it is locally unstable [25–29].

### A. Regular random graphs

For RR graphs the BP fixed point is easy to determine, namely all  $\tilde{q}_{i \rightarrow j}^0 = 1 - a$  and  $\tilde{q}_{i \rightarrow j}^i = b$ , with  $a$  and  $b$  computed according to Eq. (A1) of Appendix A. We can then write an iterative equation of perturbation as

$$\begin{bmatrix} \epsilon_{i \rightarrow j}^0 \\ \epsilon_{i \rightarrow j}^i \end{bmatrix} = \mathbf{J} \begin{bmatrix} \sum_{k \in \partial i \setminus j} \epsilon_{k \rightarrow i}^0 \\ \sum_{k \in \partial i \setminus j} \epsilon_{k \rightarrow i}^i \end{bmatrix}, \quad (17)$$

where

$$\mathbf{J} = \begin{bmatrix} \frac{\partial q_{i \rightarrow j}^0}{\partial q_{k \rightarrow i}^0} & \frac{\partial q_{i \rightarrow j}^0}{\partial q_{k \rightarrow i}^i} \\ \frac{\partial q_{i \rightarrow j}^i}{\partial q_{k \rightarrow i}^0} & \frac{\partial q_{i \rightarrow j}^i}{\partial q_{k \rightarrow i}^i} \end{bmatrix} \quad (18)$$

is a  $2 \times 2$  matrix evaluated at the BP fixed point, whose largest absolute eigenvalue is denoted as  $\lambda$ . It is reasonable to assume that the perturbations  $\epsilon_{i \rightarrow j}^0$  and  $\epsilon_{i \rightarrow j}^i$  follow the distributions with mean value 0 and variance  $\sigma_0^2$  and  $\sigma_r^2$ , respectively. Then the mean values of  $\sum_{k \in \partial i \setminus j} \epsilon_{k \rightarrow i}^0$  and  $\sum_{k \in \partial i \setminus j} \epsilon_{k \rightarrow i}^i$  are still 0 and their variances are  $(K - 1)\sigma_0^2$  and  $(K - 1)\sigma_r^2$ , respectively. After one iteration with Eq. (17) the variance of  $\epsilon_{i \rightarrow j}^0$  and  $\epsilon_{i \rightarrow j}^i$  must not exceed  $\lambda^2(K - 1)\sigma_0^2$  and  $\lambda^2(K - 1)\sigma_r^2$ . Considering that the perturbation should shrink to 0 in the case of local stability, we have the local stability criterion that  $(K - 1)\lambda^2 < 1$ .

We have checked that the results obtained by such a stability analysis are identical to those obtained by the alternative method of the next subsection.

### B. Erdős-Rényi random graphs

Because of the degree dispersion in the ER graph ensemble, the analytical method of the preceding subsection is not applicable here. Therefore, we can only measure the amplitude of the perturbations during the BP iteration and then figure out the region where the RS mean-field theory is locally stable. Following Ref. [28], this numerical procedure starts

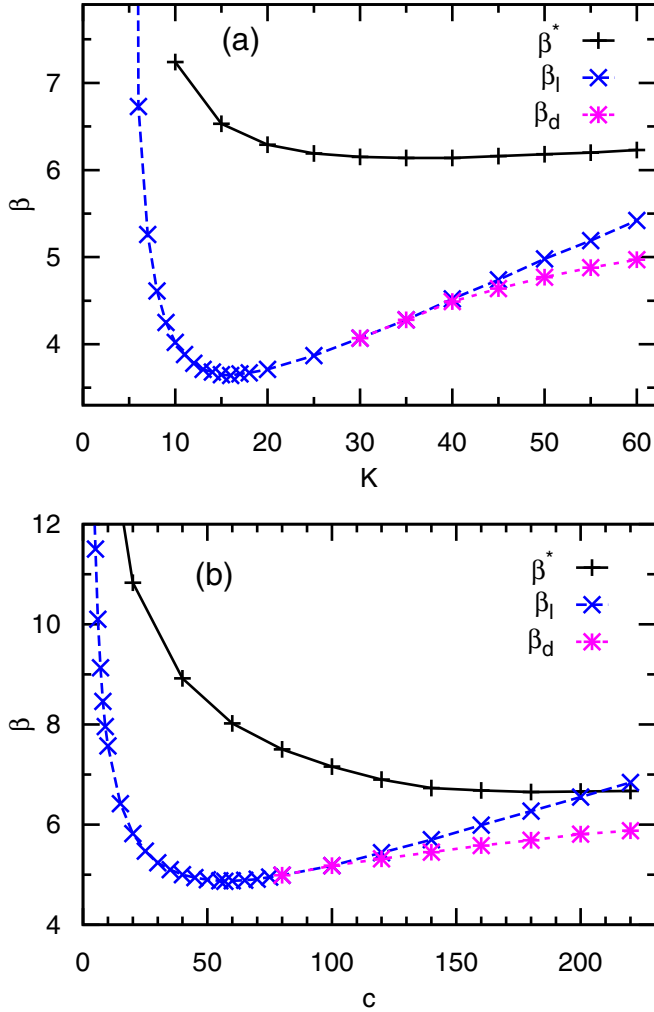


FIG. 1. The critical inverse temperature  $\beta_l$  of local stability of the RS mean-field theory, the inverse temperature  $\beta^*$  at which the RS entropy density approaches zero, and the dynamical transition inverse temperature  $\beta_d$ . (a) The RR graph ensemble with vertex degree  $K$ ; (b) the ER graph ensemble with mean vertex degree  $c$ .

from running the RS population dynamics sufficiently long to reach a steady state. Then a replica of the whole population is created to get two identical populations, and one of them is then perturbed slightly. Finally, we continue to perform the RS population dynamics simulations starting from these two initial populations using the same sequence of random numbers. In case the two populations converge to each other, we regard the RS mean-field theory to be locally stable, and otherwise it is regarded as locally unstable.

### C. Local stability results

The critical inverse temperature  $\beta_l$  of local stability is shown in Fig. 1 for the RR and ER network ensembles. To make comparison easier, we plot in this figure also the inverse temperature  $\beta^*$ , at which the RS entropy density reaches zero, and the critical inverse temperature  $\beta_d$ , at which the dynamical spin-glass transitions occurs (see Sec. IV).

The inverse temperature  $\beta_l$  is not a monotonic function of the degree  $K$  (for RR graphs) or the mean degree  $c$  (for ER

graphs); it first decreases with  $K$  or  $c$  and then slowly increases as  $K$  goes beyond 16 or  $c$  goes beyond 57. When  $K < 35$  or  $c < 100$ ,  $\beta_l$  coincides with the dynamical transition point  $\beta_d$ , but  $\beta_l > \beta_d$  for larger values of  $K$  or  $c$ .

We also find that  $\beta_l > \beta^*$  at sufficiently large  $K$  or  $c$  values, which means that the RS mean-field theory is still locally stable even if it predicts a negative entropy. This observation clearly demonstrates that  $\beta_l$  should only be treated as an upper bound of the inverse temperatures  $\beta$  at which the RS mean-field theory is physically plausible. Indeed, the property that the RS mean-field theory is locally stable at certain  $\beta < \beta_l$  does not mean the iteration of the BP equation (8) on single graph instances will necessarily converge to a fixed point.

## IV. DYNAMICAL AND STATIC PHASE TRANSITIONS

We now investigate spin-glass phase transitions in the model (3). The 1RSB mean-field theory described here is applicable to different random graph ensembles, but we carry out numerical computations mainly on the RR ensemble.

### A. First-step replica-symmetry-breaking theory

We first give a brief review of the 1RSB mean-field theory of spin glasses [18,19]. According to this theory, at sufficiently high inverse temperatures the space of legal configurations may break into exponentially many subspaces, each of which corresponds to a macroscopic state of the system and contains a set of relatively similar legal configurations. In this subsection we discuss the system at the level of macroscopic states. The partition function of macroscopic state  $\alpha$  is defined as

$$Z_\alpha(\beta) \equiv e^{-\beta F_\alpha} = \sum_{A \in \alpha} \exp[-\beta E(A)], \quad (19)$$

where the sum runs over all the legal configurations in  $\alpha$ , and  $F_\alpha$  is the free energy of  $\alpha$  [18,19].

We can define a Boltzmann distribution at the level of macroscopic states as

$$\mu_\alpha \equiv \frac{e^{-y F_\alpha}}{\Xi(y; \beta)}. \quad (20)$$

The parameter  $y$  is the inverse temperature at the macroscopic level, which may be different from the inverse temperature  $\beta$  at the level of microscopic configurations. The ratio between  $y$  and  $\beta$  is referred to as the Parisi parameter [19]. The quantity  $\mu_\alpha$  as defined in Eq. (20) determines the weight of state  $\alpha$  among all the macroscopic states, and the normalization constant  $\Xi(y; \beta) \equiv \sum_\alpha e^{-y F_\alpha}$  is the partition function at the level of macroscopic states, which can also be calculated by the integral

$$\Xi(y; \beta) = \int df e^{N[-yf + \Sigma(f)]}, \quad (21)$$

where  $f$  is the free-energy density of a macroscopic state, and  $\Sigma(f)$ , the complexity, is the entropy density of macroscopic states with free-energy density  $f$ . A nonzero complexity value is taken as a signature that the system is in a spin-glass phase [30]. We can define the grand free energy  $G(y; \beta)$  of the system

as

$$G(y; \beta) \equiv -\frac{1}{y} \ln \Xi(y; \beta). \quad (22)$$

The mean free energy among different macroscopic states is defined as  $\langle F \rangle \equiv \sum_{\alpha} \mu_{\alpha} F_{\alpha}$ . In the thermodynamic limit  $N \rightarrow \infty$ , the macroscopic states with the free-energy density  $f^* = \text{argmax}_f [-yf + \Sigma(f)]$  dominate the partition function  $\Xi(y; \beta)$ , and then  $G(y; \beta) = N[f^* - \Sigma(f^*)/y]$  and  $\langle F \rangle = Nf^*$ . Therefore the complexity is obtained through

$$\Sigma = \frac{y}{N} [\langle F \rangle - G]. \quad (23)$$

For a given edge  $(i, j)$ , when there are many macroscopic states, the cavity message  $q_{i \rightarrow j}$  from vertex  $i$  to vertex  $j$  may differ in different macroscopic states. The distribution of this message among all the macroscopic states is denoted as  $Q_{i \rightarrow j}[q_{i \rightarrow j}]$ . Under the distribution of Eq. (20) and for random graphs, we have the following self-consistent equation for  $Q_{i \rightarrow j}[q_{i \rightarrow j}]$ , which is referred to as the survey propagation (SP) equation [18,31]:

$$Q_{i \rightarrow j}[q_{i \rightarrow j}] = \frac{1}{\Xi_{i \rightarrow j}} \int \prod_{k \in \partial i \setminus j} \mathcal{D}q_{k \rightarrow i} Q_{k \rightarrow i}[q_{k \rightarrow i}] e^{-y f_{i \rightarrow j}} \times \delta[q_{i \rightarrow j} - b(\{q_{k \rightarrow i}\})], \quad (24)$$

where  $f_{i \rightarrow j}$  is the free-energy change associated with the interactions of vertex  $i$  with the vertices in the set  $\partial i \setminus j$ ,

$$f_{i \rightarrow j} = -\frac{1}{\beta} \ln z_{i \rightarrow j} \quad (25)$$

with  $z_{i \rightarrow j}$  computed through Eq. (9); and the normalization constant  $\Xi_{i \rightarrow j}$  is

$$\Xi_{i \rightarrow j} = \int \prod_{k \in \partial i \setminus j} \mathcal{D}q_{k \rightarrow i} Q_{k \rightarrow i}[q_{k \rightarrow i}] e^{-y f_{i \rightarrow j}}. \quad (26)$$

After a fixed-point solution of Eq. (24) is obtained, the grand free energy  $G$  and the mean free energy  $\langle F \rangle$  can be computed, respectively, through

$$G = \sum_{i=1}^N g_i - \sum_{(i,j) \in \mathcal{G}} g_{ij}, \quad (27)$$

$$\langle F \rangle = \sum_{i=1}^N \langle f_i \rangle - \sum_{(i,j) \in \mathcal{G}} \langle f_{ij} \rangle. \quad (28)$$

In these equations  $g_i$  and  $\langle f_i \rangle$  are the grand free energy and mean free energy contributions from vertex  $i$ , while  $g_{ij}$  and  $\langle f_{ij} \rangle$  are the corresponding contributions from edge  $(i, j)$ . Their explicit expressions are

$$g_i = -\frac{1}{y} \log \left[ \int \prod_{j \in \partial i} \mathcal{D}q_{j \rightarrow i} Q_{j \rightarrow i}[q_{j \rightarrow i}] e^{-y f_i} \right], \quad (29)$$

$$g_{ij} = -\frac{1}{y} \log \left[ \int \mathcal{D}q_{j \rightarrow i} \mathcal{D}q_{i \rightarrow j} Q_{j \rightarrow i}[q_{j \rightarrow i}] \times Q_{i \rightarrow j}[q_{i \rightarrow j}] e^{-y f_{ij}} \right], \quad (30)$$

$$\langle f_i \rangle = \frac{\int \prod_{j \in \partial i} \mathcal{D}q_{j \rightarrow i} Q_{j \rightarrow i}[q_{j \rightarrow i}] f_i e^{-y f_i}}{\int \prod_{j \in \partial i} \mathcal{D}q_{j \rightarrow i} Q_{j \rightarrow i}[q_{j \rightarrow i}] e^{-y f_i}}, \quad (31)$$

$$\langle f_{ij} \rangle = \frac{\int \mathcal{D}q_{j \rightarrow i} \mathcal{D}q_{i \rightarrow j} Q_{j \rightarrow i}[q_{j \rightarrow i}] Q_{i \rightarrow j}[q_{i \rightarrow j}] f_{ij} e^{-y f_{ij}}}{\int \mathcal{D}q_{j \rightarrow i} \mathcal{D}q_{i \rightarrow j} Q_{j \rightarrow i}[q_{j \rightarrow i}] Q_{i \rightarrow j}[q_{i \rightarrow j}] e^{-y f_{ij}}}. \quad (32)$$

## B. Special case of $y = \beta$

We now consider the most natural value of  $y = \beta$  (the inverse temperature at the level of macroscopic states being equal to that at the level of microscopic configurations) and investigate spin-glass phase transitions. In order to simplify the 1RSB mean-field theory at  $y = \beta$ , we introduce a coarse-grained probability as

$$q_{i \rightarrow j}^X \equiv \sum_{l \in \partial i \setminus j} q_{i \rightarrow j}^l, \quad (33)$$

where the superscript ‘‘X’’ indicates that the state  $A_i$  of vertex  $i$  is neither  $i$  nor 0. The quantity  $q_{i \rightarrow j}^X$  is the probability that, in the absence of vertex  $j$ , vertex  $i$  is occupied ( $A_i > 0$ ) but it is not a root ( $A_i \neq i$ ).

Following the work of Mézard and Montanari [32] we define  $\bar{q}_{i \rightarrow j} \equiv (\bar{q}_{i \rightarrow j}^0, \bar{q}_{i \rightarrow j}^i, \bar{q}_{i \rightarrow j}^X)$  as the mean value of  $q_{i \rightarrow j}$  among all the macroscopic states:

$$\bar{q}_{i \rightarrow j}^0 = \int \mathcal{D}q_{i \rightarrow j} Q_{i \rightarrow j}[q_{i \rightarrow j}] q_{i \rightarrow j}^0, \quad (34a)$$

$$\bar{q}_{i \rightarrow j}^i = \int \mathcal{D}q_{i \rightarrow j} Q_{i \rightarrow j}[q_{i \rightarrow j}] q_{i \rightarrow j}^i, \quad (34b)$$

$$\bar{q}_{i \rightarrow j}^X = \int \mathcal{D}q_{i \rightarrow j} Q_{i \rightarrow j}[q_{i \rightarrow j}] q_{i \rightarrow j}^X. \quad (34c)$$

$\bar{q}_{i \rightarrow j}^0$  and  $\bar{q}_{i \rightarrow j}^i$  are the mean cavity probabilities of vertex  $i$  being in state  $A_i = 0$  and  $A_i = i$ , while  $\bar{q}_{i \rightarrow j}^X$  is the mean cavity probability of taking states different from  $A_i = 0$  and  $A_i = i$ . In addition, we define three auxiliary conditional probability functionals as

$$Q_{i \rightarrow j}^0[q_{i \rightarrow j}] \equiv \frac{q_{i \rightarrow j}^0 Q_{i \rightarrow j}[q_{i \rightarrow j}]}{\bar{q}_{i \rightarrow j}^0}, \quad (35a)$$

$$Q_{i \rightarrow j}^i[q_{i \rightarrow j}] \equiv \frac{q_{i \rightarrow j}^i Q_{i \rightarrow j}[q_{i \rightarrow j}]}{\bar{q}_{i \rightarrow j}^i}, \quad (35b)$$

$$Q_{i \rightarrow j}^X[q_{i \rightarrow j}] \equiv \frac{q_{i \rightarrow j}^X Q_{i \rightarrow j}[q_{i \rightarrow j}]}{\bar{q}_{i \rightarrow j}^X}. \quad (35c)$$

$Q_{i \rightarrow j}^0[q_{i \rightarrow j}]$ ,  $Q_{i \rightarrow j}^i[q_{i \rightarrow j}]$ , and  $Q_{i \rightarrow j}^X[q_{i \rightarrow j}]$  are the distribution functionals for the cavity message  $q_{i \rightarrow j}$  under the condition of  $A_i = 0$ ,  $A_i = i$ , and  $A_i \notin \{0, i\}$ , respectively. It is easy to verify the identity that

$$Q_{i \rightarrow j}[q_{i \rightarrow j}] = \bar{q}_{i \rightarrow j}^0 Q_{i \rightarrow j}^0[q_{i \rightarrow j}] + \bar{q}_{i \rightarrow j}^i Q_{i \rightarrow j}^i[q_{i \rightarrow j}] + \bar{q}_{i \rightarrow j}^X Q_{i \rightarrow j}^X[q_{i \rightarrow j}]. \quad (36)$$

At the special case of  $y = \beta$ , by inserting the SP equation (24) into Eq. (34), we obtain that the mean cavity probability

$\bar{q}_{i \rightarrow j}$  also obeys the BP equation (8),

$$\bar{q}_{i \rightarrow j} = b(\{\bar{q}_{k \rightarrow i} : k \in \partial i \setminus j\}). \quad (37)$$

In other words, the mean cavity probabilities  $\{\bar{q}_{i \rightarrow j}\}$  can be computed without the need of computing the probability functionals  $\{Q_{i \rightarrow j}[q_{i \rightarrow j}]\}$ . We now exploit this nice property in combination with Eq. (35) to greatly simplify the numerical difficulty of implementing the 1RSB mean-field theory [32,33].

After inserting Eq. (24) into Eq. (35), we find that the three auxiliary probability functionals obey the following self-consistent equations:

$$\begin{aligned} Q_{i \rightarrow j}^0[q_{i \rightarrow j}] &= \prod_{k \in \partial i \setminus j} \int \mathcal{D}q_{k \rightarrow i} [\bar{q}_{k \rightarrow i}^0 Q_{k \rightarrow i}^0[q_{k \rightarrow i}] \\ &\quad + \bar{q}_{k \rightarrow i}^k Q_{k \rightarrow i}^k[q_{k \rightarrow i}] + \bar{q}_{k \rightarrow i}^X Q_{k \rightarrow i}^X[q_{k \rightarrow i}]] \\ &\quad \times \delta[q_{i \rightarrow j} - b(\{q_{k \rightarrow i}\})], \end{aligned} \quad (38a)$$

$$\begin{aligned} Q_{i \rightarrow j}^i[q_{i \rightarrow j}] &= \prod_{k \in \partial i \setminus j} \int \mathcal{D}q_{k \rightarrow i} \left[ \frac{\bar{q}_{k \rightarrow i}^0}{\bar{q}_{k \rightarrow i}^0 + \bar{q}_{k \rightarrow i}^k} Q_{k \rightarrow i}^0[q_{k \rightarrow i}] \right. \\ &\quad \left. + \frac{\bar{q}_{k \rightarrow i}^k}{\bar{q}_{k \rightarrow i}^0 + \bar{q}_{k \rightarrow i}^k} Q_{k \rightarrow i}^k[q_{k \rightarrow i}] \right] \\ &\quad \times \delta[q_{i \rightarrow j} - b(\{q_{k \rightarrow i}\})], \end{aligned} \quad (38b)$$

$$\begin{aligned} Q_{i \rightarrow j}^X[q_{i \rightarrow j}] &= \sum_{k \in \partial i \setminus j} \omega_{k \rightarrow i} \int \mathcal{D}q_{k \rightarrow i} \left[ \frac{\bar{q}_{k \rightarrow i}^k}{\bar{q}_{k \rightarrow i}^k + \bar{q}_{k \rightarrow i}^X} \right. \\ &\quad \left. \times Q_{k \rightarrow i}^k[q_{k \rightarrow i}] + \frac{\bar{q}_{k \rightarrow i}^X}{\bar{q}_{k \rightarrow i}^k + \bar{q}_{k \rightarrow i}^X} Q_{k \rightarrow i}^X[q_{k \rightarrow i}] \right] \\ &\quad \times \prod_{l \in \partial i \setminus j, k} \int \mathcal{D}q_{l \rightarrow i} \left[ \frac{\bar{q}_{l \rightarrow i}^0}{\bar{q}_{l \rightarrow i}^0 + \bar{q}_{l \rightarrow i}^l} Q_{l \rightarrow i}^0[q_{l \rightarrow i}] \right. \\ &\quad \left. + \frac{\bar{q}_{l \rightarrow i}^l}{\bar{q}_{l \rightarrow i}^0 + \bar{q}_{l \rightarrow i}^l} Q_{l \rightarrow i}^l[q_{l \rightarrow i}] \right] \\ &\quad \times \delta[q_{i \rightarrow j} - b(\{q_{k \rightarrow i}\})]. \end{aligned} \quad (38c)$$

In Eq. (38c) the probability  $w_{k \rightarrow i}$  is determined as

$$\omega_{k \rightarrow i} = \frac{(1 - \bar{q}_{k \rightarrow i}^0) \prod_{l \in \partial i \setminus j, k} [\bar{q}_{l \rightarrow i}^0 + \bar{q}_{l \rightarrow i}^l]}{\sum_{m \in \partial i \setminus j} (1 - \bar{q}_{m \rightarrow i}^0) \prod_{l \in \partial i \setminus j, m} [\bar{q}_{l \rightarrow i}^0 + \bar{q}_{l \rightarrow i}^l]}, \quad (39)$$

and it can be understood as the probability of choosing vertex  $k$  among all the vertices in the set  $\partial i \setminus j$ . The iterative equation (38) avoids the difficulty of reweighted sampling in the original SP equation (24).

For a given graph instance  $\mathcal{G}$ , we describe the statistical property of vertex  $i$  in the absence of the neighboring vertex  $j$  by the mean cavity probability function  $\bar{q}_{i \rightarrow j}$  and the three conditional probability functionals  $Q_{i \rightarrow j}^0[q]$ ,  $Q_{i \rightarrow j}^i[q]$ , and  $Q_{i \rightarrow j}^X[q]$ , each of which is represented by a set of sampled cavity probabilities  $q_{i \rightarrow j}$ . We first iterate the BP equation (37) a number of rounds to bring the set of mean cavity probabilities  $\{\bar{q}_{i \rightarrow j}\}$  to the fixed point (or at least close to the fixed point). Then Eq. (38) is iterated to drive all the conditional

probability functionals to their steady states. For example, to update  $Q_{i \rightarrow j}^X[q_{i \rightarrow j}]$  using Eq. (38c), we (i) choose a vertex  $k \in \partial i \setminus j$  with probability  $\omega_{k \rightarrow i}$ , and then (ii) draw a cavity probability  $q_{k \rightarrow i}$  from  $Q_{k \rightarrow i}^k[q]$  with probability  $\frac{\bar{q}_{k \rightarrow i}^k}{\bar{q}_{k \rightarrow i}^k + \bar{q}_{k \rightarrow i}^X}$  or from  $Q_{k \rightarrow i}^X[q]$  with the remaining probability  $\frac{\bar{q}_{k \rightarrow i}^X}{\bar{q}_{k \rightarrow i}^k + \bar{q}_{k \rightarrow i}^X}$ , and (iii) for each of the other vertices  $l \in \partial i \setminus j, k$  select a cavity probability  $q_{l \rightarrow i}$  from  $Q_{l \rightarrow i}^0[q_{l \rightarrow i}]$  with probability  $\frac{\bar{q}_{l \rightarrow i}^0}{\bar{q}_{l \rightarrow i}^0 + \bar{q}_{l \rightarrow i}^l}$  or from  $Q_{l \rightarrow i}^l[q_{l \rightarrow i}]$  with the remaining probability  $\frac{\bar{q}_{l \rightarrow i}^l}{\bar{q}_{l \rightarrow i}^0 + \bar{q}_{l \rightarrow i}^l}$ , and finally (iv) generate a new cavity probability  $q_{i \rightarrow j}$  using the BP equation (8) and replace a randomly chosen old cavity probability of the set representing  $Q_{i \rightarrow j}^X[q_{i \rightarrow j}]$  by this new one. The other two conditional probability functionals  $Q_{i \rightarrow j}^0[q_{i \rightarrow j}]$  and  $Q_{i \rightarrow j}^i[q_{i \rightarrow j}]$  are updated through the same numerical procedure.

At  $y = \beta$  the computation of the grand free energy density  $g \equiv G/N$  and the mean free energy density  $\langle f \rangle \equiv \langle F \rangle/N$  can also be carried out without reweighting among the different macroscopic states. We list in Appendix B the explicit mean-field expressions for computing  $g$  and  $\langle f \rangle$ .

The initial condition for the iterative equation (38) is chosen to be the following set of Dirac  $\delta$ -formed probability functionals:

$$Q_{i \rightarrow j}^0[q_{i \rightarrow j}] = \delta(q_{i \rightarrow j}^0 - 1) \delta(q_{i \rightarrow j}^i) \delta(q_{i \rightarrow j}^X), \quad (40a)$$

$$Q_{i \rightarrow j}^i[q_{i \rightarrow j}] = \delta(q_{i \rightarrow j}^0) \delta(q_{i \rightarrow j}^i - 1) \delta(q_{i \rightarrow j}^X), \quad (40b)$$

$$Q_{i \rightarrow j}^X[q_{i \rightarrow j}] = \delta(q_{i \rightarrow j}^0) \delta(q_{i \rightarrow j}^i) \delta(q_{i \rightarrow j}^X - 1). \quad (40c)$$

According to the theoretical analysis in Ref. [32], if the conditional probability functionals (35) starting from this initial condition converge to the trivial fixed point

$$\begin{aligned} Q_{i \rightarrow j}^0[q_{i \rightarrow j}] &= Q_{i \rightarrow j}^i[q_{i \rightarrow j}] = Q_{i \rightarrow j}^X[q_{i \rightarrow j}] \\ &= \delta(q_{i \rightarrow j}^0 - \bar{q}_{i \rightarrow j}^0) \delta(q_{i \rightarrow j}^i - \bar{q}_{i \rightarrow j}^i) \\ &\quad \times \delta(q_{i \rightarrow j}^X - \bar{q}_{i \rightarrow j}^X), \end{aligned} \quad (41)$$

the system is then in the ergodic phase with a unique equilibrium macroscopic state (complexity  $\Sigma = 0$ ). If the conditional probability functionals (35) converges to a fixed point that differs from Eq. (41), the system is then in the ergodicity-breaking spin-glass phase with exponentially many equilibrium macroscopic states (complexity  $\Sigma \neq 0$ ). The critical inverse temperature  $\beta_d$ , at which the complexity  $\Sigma$  starts to deviate from zero, marks the onset of the spin-glass phase. In the literature  $\beta_d$  is referred to as the dynamical or clustering transition point [19]. The critical inverse temperature  $\beta_s$ , at which the complexity  $\Sigma$  starts to be negative, is referred to as the static or condensation transition point [19].

### C. Critical inverse temperatures $\beta_d$ and $\beta_s$

At  $y = \beta$ , we can determine the ensemble-averaged complexity value  $\Sigma$  as a function of the inverse temperature  $\beta$  by iterating Eq. (38) through population dynamics [18,28,31,33,34]. The technical details are given in Appendix C, and here we describe the numerical results for RR and ER graph ensembles.

The inverse temperature  $\beta_d$  of dynamical transition is compared with the critical inverse temperature  $\beta_l$  of RS local stability in Fig. 1. Similar to  $\beta_l$ , we see that  $\beta_d$  is not a monotonic function of the (mean) vertex mean degree. For the RR ensemble,  $\beta_d$  first decreases with the degree  $K$  and reaches the minimum value of  $\beta_d \approx 3.64$  at  $K = 16$ , then  $\beta_d$  increases slowly with  $K$ . For  $K < 35$  the values of  $\beta_d$  and  $\beta_l$

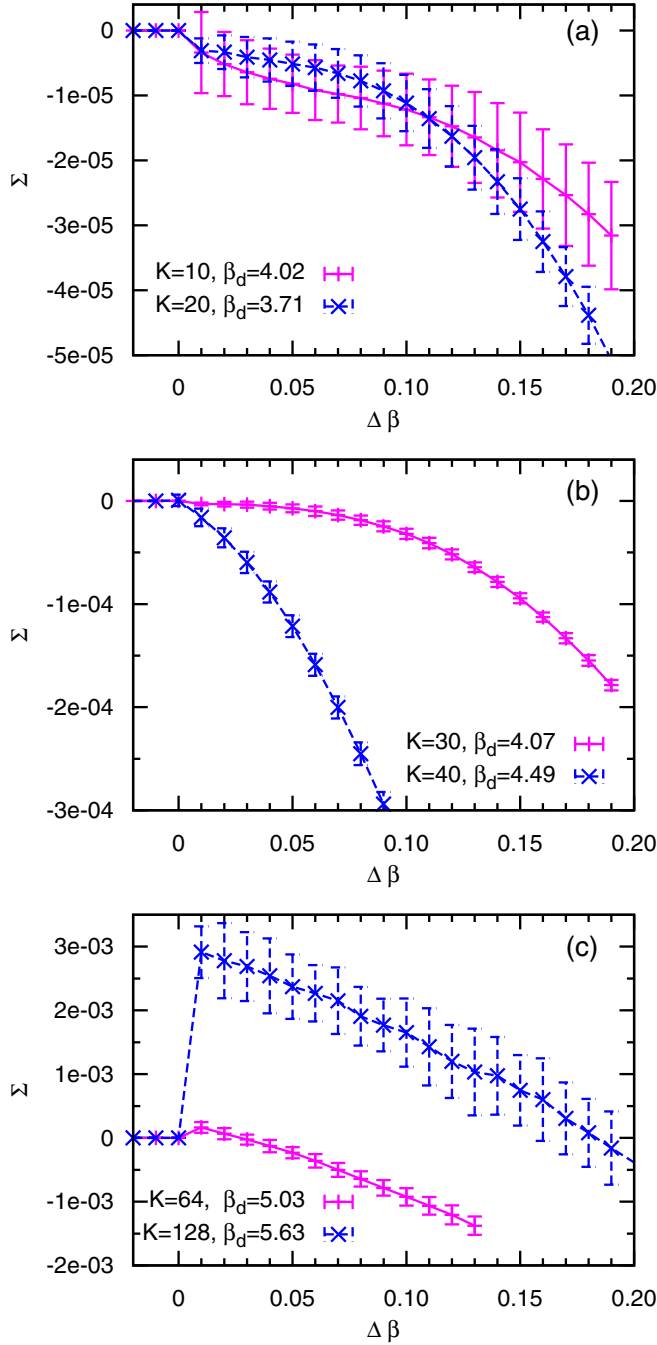


FIG. 2. Complexity  $\Sigma$  as a function of inverse temperature  $\beta$  in the vicinity of the dynamical transition point  $\beta_d$ , with  $\Delta\beta \equiv (\beta - \beta_d)$ . Results are obtained by population dynamics at  $y = \beta$  for the RR graph ensemble. (a) Degree  $K = 10$  ( $\beta_d \approx 4.02$ ) and  $K = 20$  ( $\beta_d \approx 3.71$ ). (b)  $K = 30$  ( $\beta_d \approx 4.07$ ) and  $K = 40$  ( $\beta_d \approx 4.49$ ). (c)  $K = 64$  ( $\beta_d \approx 5.03$ ) and  $K = 128$  ( $\beta_d \approx 5.63$ ).

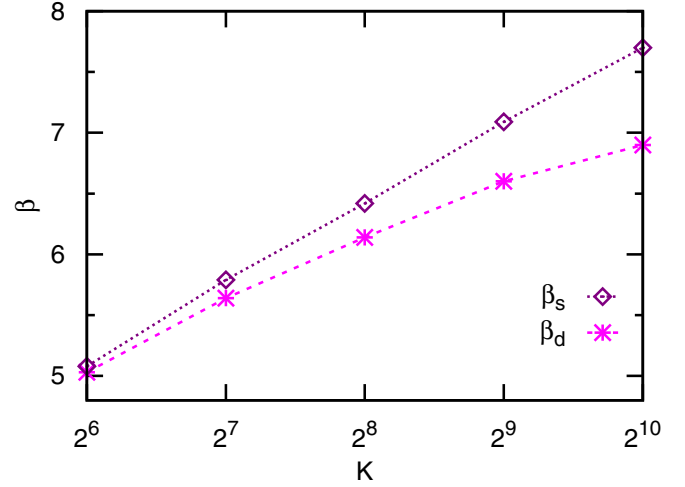


FIG. 3. The dynamical transition inverse temperature  $\beta_d$  (star symbols) and the static transition inverse temperature  $\beta_s$  (diamond symbols) for the RR graph ensemble of vertex degree  $K$ .

are indistinguishable, while  $\beta_d$  becomes noticeably lower than  $\beta_l$  at  $K > 35$ . For the ER ensemble,  $\beta_d$  reaches the minimum value at mean degree  $c \approx 57$ , and it becomes noticeably lower than  $\beta_l$  as  $c$  exceeds 100.

The complexity  $\Sigma$  computed at  $y = \beta$  in the vicinity of the dynamical transition point  $\beta_d$  is shown in Fig. 2 for the RR graph ensemble. When the vertex degree  $K$  is sufficiently small ( $K < 60$ ),  $\Sigma$  changes from  $\Sigma = 0$  to  $\Sigma < 0$  as  $\beta$  exceeds  $\beta_d$ , indicating that in the spin-glass phase the equilibrium configuration space is dominated by only a few macroscopic states [17,33]. The critical inverse temperature  $\beta_s$  of static spin-glass transition therefore coincides with  $\beta_d$ . However, when  $K > 60$ , the complexity  $\Sigma$  jumps from zero to a positive value at  $\beta = \beta_d$  [see Fig. 2(c)], suggesting that the equilibrium configuration space breaks into an exponential number of subspaces (macroscopic states) at  $\beta_d$  [30,33]. The complexity then gradually decreases with  $\beta$  and becomes negative as  $\beta$  exceeds the critical value  $\beta_s$  of static transition. As shown in

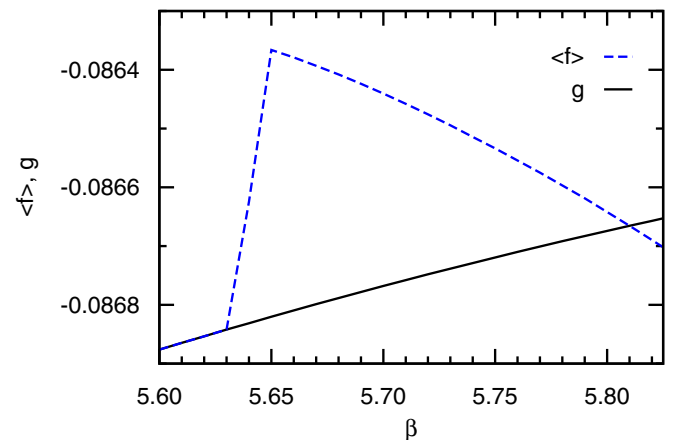


FIG. 4. The mean free energy density  $\langle f \rangle$  and the grand free energy density  $g$  for the RR graph ensemble of vertex degree  $K = 128$ . For this system  $\beta_d \approx 5.64$  and  $\beta_s \approx 5.81$ .

Fig. 3, the gap between  $\beta_d$  and  $\beta_s$  enlarges with the vertex degree  $K$  for  $K > 60$ . We notice that  $\beta_s$  may be lower than the critical value  $\beta_l$  of the RS local stability (for example at  $K = 64$ ,  $\beta_s \approx 5.055$  while  $\beta_l \approx 5.5$ ).

At  $\beta < \beta_d$  the system has only a unique equilibrium macroscopic state, therefore the complexity  $\Sigma$  is exactly zero and the mean free energy density  $\langle f \rangle$  is identical to the grand free energy density  $g$  (see Fig. 4 for the particular case of  $K = 128$ ). At each inverse temperature of  $\beta \in (\beta_d, \beta_s)$  the system has an exponential number ( $\approx e^{N\Sigma}$ ) of equilibrium macroscopic states. The mean free energy density  $\langle f \rangle$  of a macroscopic state is larger than the grand free energy density  $g$ , with  $g = \langle f \rangle - \frac{1}{\beta} \Sigma$ . Notice that the grand free energy density  $g$  changes smoothly at  $\beta_d$  while  $\langle f \rangle$  has a discontinuity (Fig. 4).  $\Sigma = 0$  and the mean free energy density  $\langle f \rangle$  is identical to the grand free energy density  $g$  (see Fig. 4 for the case of  $K = 128$ ). At  $\beta = \beta_d$  the complexity  $\Sigma$  jumps to a positive value and the equilibrium configuration space breaks into  $O(e^{N\Sigma})$  clusters (macroscopic states) with mean free energy density  $\langle f \rangle$  larger than the grand free energy density  $g$ . Notice that the grand free energy density  $g$  changes smoothly at  $\beta_d$  while  $\langle f \rangle$  has a discontinuity (Fig. 4). In the interval of  $\beta_d < \beta < \beta_s$ , the mean free energy density  $\langle f \rangle$  of a macroscopic state decreases with  $\beta$  while the grand free energy density  $g$  of the whole system increases with  $\beta$ . At  $\beta = \beta_s$ ,  $\langle f \rangle$  becomes equal to  $g$  and the complexity  $\Sigma$  reaches zero. In the whole region of  $\beta > \beta_s$  the system is dominated by a few macroscopic states.

We have also investigated the ER graph ensemble by the same method. For this ensemble we find that the complexity  $\Sigma$  (at  $y = \beta$ ) becomes negative as  $\beta$  increases from  $\beta_d$  for all the considered mean vertex degrees up to  $c = 512$ , indicating that  $\beta_s = \beta_d$ . It is still unclear to us whether the static transition point  $\beta_s$  will be distinct from the dynamical transition point  $\beta_d$  at larger values of mean degree  $c$ .

## V. ZERO-TEMPERATURE ( $\beta \rightarrow \infty$ ) LIMIT

At inverse temperature  $\beta > \beta_s$ , only very few macroscopic states (those with the lowest free-energy density) are important for the equilibrium property of the system. In this section we consider the limiting case of  $\beta \rightarrow \infty$  which corresponds to the minimum FVS problem. At this limit the 1RSB mean-field theory can be simplified to a considerable extent [31,35–37]. The corresponding infinite- $\beta$  SP equation but with finite value of  $y$  is referred to as SP( $y$ ).

Before deriving the SP( $y$ ) equation, we first need to obtain the zero-temperature limit of the BP equation (8). This limit is very closely related to the max-product or min-sum algorithm [18,36,38]. It is convenient for us to rewrite the cavity messages as

$$q_{i \rightarrow j}^0 \equiv e^{-\beta \gamma_{i \rightarrow j}}, \quad (42a)$$

$$q_{i \rightarrow j}^0 + q_{i \rightarrow j}^i \equiv e^{-\beta \rho_{i \rightarrow j}}, \quad (42b)$$

$$\frac{1 - q_{i \rightarrow j}^0}{q_{i \rightarrow j}^0 + q_{i \rightarrow j}^i} \equiv e^{-\beta \eta_{i \rightarrow j}}. \quad (42c)$$

At  $\beta \rightarrow \infty$ , we obtain from Eq. (8) the following iterative equations for  $\gamma_{i \rightarrow j}$ ,  $\rho_{i \rightarrow j}$ , and  $\eta_{i \rightarrow j}$ :

$$\gamma_{i \rightarrow j} = 1 - \min \left( 1, \sum_{k \in \partial i \setminus j} \rho_{k \rightarrow i} + \min(0, \{\eta_{k \rightarrow i}\}_{k \in \partial i \setminus j}) \right), \quad (43a)$$

$$\rho_{i \rightarrow j} = \min \left( 1, \sum_{k \in \partial i \setminus j} \rho_{k \rightarrow i} \right) + \gamma_{i \rightarrow j} - 1, \quad (43b)$$

$$\eta_{i \rightarrow j} = \min(0, \{\eta_{k \rightarrow i}\}_{k \in \partial i \setminus j}) - \min \left( 0, 1 - \sum_{k \in \partial i \setminus j} \rho_{k \rightarrow i} \right). \quad (43c)$$

Notice that  $0 \leq \gamma_{i \rightarrow j} \leq 1$  and  $0 \leq \rho_{i \rightarrow j} \leq 1$ . To simplify the notation we denote by  $\chi_{i \rightarrow j} \equiv \{\gamma_{i \rightarrow j}, \rho_{i \rightarrow j}, \eta_{i \rightarrow j}\}$ . The minimum BP equation (43) is then denoted as  $\chi_{i \rightarrow j} = b_\infty(\{\chi_{k \rightarrow i} : k \in \partial i \setminus j\})$ .

At  $\beta \rightarrow \infty$  the free-energy contributions  $f_i$  and  $f_{ij}$  of a vertex  $i$  and an edge have the corresponding limiting value  $f_i^\infty$  and  $f_{ij}^\infty$ :

$$f_i^\infty = \min \left( 1, \sum_{k \in \partial i} \rho_{k \rightarrow i} + \min(0, \{\eta_{k \rightarrow i}\}_{k \in \partial i}) \right), \quad (44a)$$

$$f_{ij}^\infty = \min(\gamma_{i \rightarrow j} + \gamma_{j \rightarrow i}, \rho_{i \rightarrow j} + \rho_{j \rightarrow i} + \min(\eta_{i \rightarrow j}, \eta_{j \rightarrow i})). \quad (44b)$$

At  $\beta \rightarrow \infty$  the probability functional  $Q_{i \rightarrow j}[q_{i \rightarrow j}]$  of Eq. (24) corresponds to the limiting probability functional  $Q_{i \rightarrow j}^\infty[\chi_{i \rightarrow j}]$ , and the self-consistent equation for this functional is

$$Q_{i \rightarrow j}^\infty[\chi] \propto \int \prod_{k \in \partial i \setminus j} \mathcal{D}\chi_{k \rightarrow i} Q_{k \rightarrow i}^\infty[\chi_{k \rightarrow i}] e^{-y f_{i \rightarrow j}^\infty} \times \delta[\chi_{i \rightarrow j} - b_\infty(\{\chi_{k \rightarrow i}\})], \quad (45)$$

where  $f_{i \rightarrow j}^\infty = 1 - \gamma_{i \rightarrow j}$ . At  $\beta \rightarrow \infty$  the grand free energy density  $g$  and the mean free energy density  $\langle f \rangle$  can be computed accordingly, and we can then determine the zero-temperature complexity  $\Sigma$  by

$$\Sigma = y(\langle f \rangle - g). \quad (46)$$

The infinite- $\beta$  1RSB mean-field theory is applicable on single graph instances. To obtain ensemble-averaged results, we can carry out 1RSB population dynamics simulations on a given random graph ensemble. We refer to this population dynamics approach as the 1RSB-P method and describe some essential simulation details in the first part of Appendix D.

Figure 5(a) shows how the infinite- $\beta$  complexity  $\Sigma$  changes with the reweighting parameter  $y$  for the RR graph ensemble of degree  $K$ . We see that  $\Sigma$  reaches a maximum value at  $y \approx 3$  and then decreases with  $y$  and becomes negative as  $y$  exceeds certain threshold value  $y^*$ . Since  $\Sigma = 0$  at  $y = y^*$ , we take the mean free energy density  $\langle f \rangle$  computed at  $y^*$  as the minimum energy density  $e_0$  of the system. For example, at  $K = 15$ , we have  $y^* \approx 4.32$  and the FVS minimum energy density is predicted to be  $e_0 = 0.636296$ . The predicted minimum

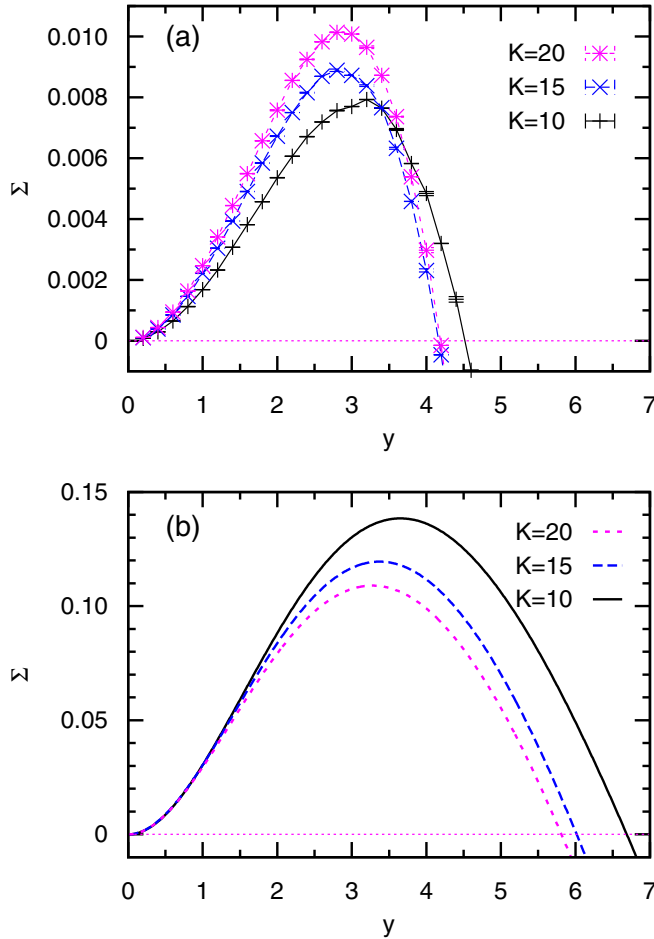


FIG. 5. The  $\beta \rightarrow \infty$  complexity  $\Sigma$  of the RR graph ensemble as a function of the reweighting parameter  $\gamma$ . The vertex degrees are  $K = 10, 15$ , and  $30$ . Results in (a) are obtained using the IRSB-P method (without using the integer-field assumption), while results in (b) are obtained by the IRSB-A method (adopting the integer-field assumption).

energy density  $e_0$  for the RR graph ensemble of  $K \in [10, 40]$  are listed in the sixth column of Table I. These predictions are slightly larger than the predictions (the third column) of the RS mean-field theory [16], and they are very close to the results (the ninth column) obtained by the BPD algorithm on single RR graph instances [16].

Generally speaking, the quantities  $\gamma_{i \rightarrow j}$ ,  $\rho_{i \rightarrow j}$ , and  $\eta_{i \rightarrow j}$  of the SP( $\gamma$ ) equation (43) are all real-valued. However we notice that if initially all these quantities are assigned integer values, their values will keep to be integer under the iteration of Eq. (43). The 1RSB population dynamics can be much simplified under such an integer-field assumption [31, 39, 40]. For the RR graph ensemble, besides this integer-field assumption, in addition we can assume that the infinite- $\beta$  1RSB message  $\chi_{i \rightarrow j}$  is independent of the vertex indices  $i$  and  $j$ . Under these two additional assumptions the infinite- $\beta$  1RSB mean-field theory can be solved analytically (see the second part of Appendix D). We refer to this analytical approach as the IRSB-A method. Some representative curves of the complexity  $\Sigma$  obtained by this method are shown in Fig. 5(b).

Comparing Fig. 5(b) with Fig. 5(a), we notice that at a given degree  $K$  the predicted peak value of the complexity  $\Sigma$  by the IRSB-A method is much larger. This apparent discrepancy very likely is caused by the splitting of a macroscopic state into many tiny substates. When the integer-field assumption is not used (as in the IRSB-P method), most vertices  $i$  may be in an unfrozen situation within a macroscopic state and they can take different states  $A_i$ , and the internal entropy of a macroscopic state is relatively large. When the integer-field assumption is applied, the states  $A_i$  of most vertices  $i$  will have to be frozen within a macroscopic state and the internal entropy of the macroscopic state will be quite small [31, 39, 40]. A highly frozen macroscopic state under the integer-field assumption is actually only a substate of the original (largely unfrozen) macroscopic state. Consistent with this physical picture, we notice that the integer-field assumption does not lead to a shift in the ground-state energy density (see the seventh column of Table I). Therefore it is safe to estimate the ground-state energy density of the spin-glass system using the integer-field assumption, which reduces considerably the computational complication of the 1RSB mean-field theory.

Our 1RSB numerical results on the ground-state energy densities  $e_0$  of the RR graph ensembles are consistent with the rigorous lower bounds obtained in Ref. [22] and the mean-field results obtained in Ref. [6] through a different spin-glass model (see Table I). For  $K = 3$  and  $K = 4$ , the RS and 1RSB mean-field theories give identical predictions on the ground-state energy density  $e_0$ . For  $K \geq 5$  the value of  $e_0$  predicted by the 1RSB mean-field theory is slightly higher than the value predicted by the RS mean-field theory. The relative sizes of FVS solutions obtained by the heuristic BPD algorithm are very close to the predicted  $e_0$  values by the 1RSB mean-field theory, indicating that this message-passing algorithm is capable of constructing close-to-minimum feedback vertex sets for single RR graph instances [16].

Based on the iterative SP( $\gamma$ ) equation (43) we can easily implement a survey propagation-guided decimation (SPD) algorithm as a solver for the minimum FVS problem. As argued above, we can restrict the 1RSB cavity messages  $\gamma_{i \rightarrow j}$ ,  $\rho_{i \rightarrow j}$ ,  $\eta_{i \rightarrow j}$  to be integer-valued, and then the implementation details of the SPD algorithm are largely the same as those of the BPD algorithm [16]. Given that the BPD algorithm is already excellent for RR and ER random graphs, the improvement of SPD over BPD is expected to be insignificant for these two graph ensembles. But for some real-world network instances with complicated structural correlations SPD might achieve better performance than BPD.

## VI. CONCLUSION

In this paper we studied the low-temperature energy landscape property of a spin-glass model for the undirected feedback vertex set problem. Through the first-step replica-symmetry-breaking mean-field theory of spin glasses, we determined the dynamical (clustering) phase transition inverse temperature  $\beta_d$  and the static (condensation) phase transition inverse temperature  $\beta_s$  for this spin-glass model, and we also considered the zero-temperature limit of the 1RSB mean-field theory and computed the minimum FVS size for the regular random graph ensemble. Our zero-temperature

TABLE I. Theoretical and simulation results on the minimum energy density (i.e., the relative size of minimum FVS) of the RR graph ensemble.  $K$  is the vertex degree. The mathematical lower-bound (LB) was obtained in Ref. [22] through probabilistic reasoning. The RS mean-field results are obtained by three different ways: by the RS population dynamics (RS-P [16]), by the analytical formula of Appendix A (RS-A), and by the height-based spin-glass model (RS-H [6]). The 1RSB mean-field results are also obtained by three different ways: by the 1RSB population dynamics (1RSB-P), by the analytical formula of Appendix D under the integer-field assumption (1RSB-A), and by the height-based spin-glass model (1RSB-H [6]). The BPD simulation results were from Ref. [16], with each data point being an average over a single running of the BPD algorithm with fixed parameter  $\beta = 7.0$  on 98 graph instances of size  $N = 10^5$ .

K	LB [22]	RS			1RSB			BPD [16]
		RS-P [16]	RS-A	RS-H [6]	1RSB-P	1RSB-A	1RSB-H [6]	
3	$\frac{1}{4}$	$\frac{1}{4}$	$\frac{1}{4}$	$\frac{1}{4}$		$\frac{1}{4}$	$\frac{1}{4}$	0.2546(1)
4	$\frac{1}{3}$	$\frac{1}{3}$	$\frac{1}{3}$	$\frac{1}{3}$		$\frac{1}{3}$	$\frac{1}{3}$	0.33383(5)
5	0.3784	0.3784	0.3784	0.3784		0.3785	0.3785	0.38223(7)
6	0.4225	0.4230	0.4219	0.4226		0.4234	0.4227	0.42608(8)
7	0.4597	0.4615	0.4589	0.4600		0.4620	0.4602	0.4647(1)
10	0.5430	0.5467	0.542		0.5486	0.5482		0.5503(1)
15	0.6305	0.6344	0.629		0.6363	0.6370		0.6384(1)
20	0.6866	0.6898	0.686		0.6920	0.6929		0.6941(1)
25			0.725		0.7311	0.7320		
30			0.755		0.7605	0.7613		
35			0.778		0.7836	0.7841		
40			0.797		0.8020	0.8025		

survey-propagation equation (43), especially the simplified version under the additional integer-field assumption (see Appendix D), should be useful for constructing nearly optimal FVS solutions for single graph instances.

One of our major theoretical results is that, for the RR graph ensemble with vertex degree  $K > 60$ , the undirected FVS problem has two distinct phase transitions, one is dynamical in nature and occurs at inverse temperature  $\beta = \beta_d$ , the other one is static in nature and occurs at a higher  $\beta = \beta_s$ . The existence of two separate spin-glass transitions is a common feature for many-body interaction models (like the random  $K$ -satisfiability problem with  $K \geq 4$  [34] and the  $p$ -spin-glass model with  $p \geq 3$  [41,42]) and many-states systems (like the  $q$ -coloring problem with  $q \geq 4$  [38]). Such a feature has also been predicted to occur in the random vertex cover problem [29,43].

For the Erdős-Rényi graph ensemble up to mean vertex degree  $c = 512$  our 1RSB mean-field theory predicts that  $\beta_s = \beta_d$ . It is indeed surprising to observe such a difference between the ER and the RR graph ensemble, we need further evidence to confirm the validity of this observation. Maybe  $c$  needs to be very large for  $\beta_s$  to be distinct from  $\beta_d$ . One way of checking this possibility is to study the 1RSB mean-field theory at the large  $c$  limit [44,45], but we have not yet carried out such an effort in this paper.

#### ACKNOWLEDGMENTS

The authors thank Chuang Wang, Pan Zhang, and Jin-Hua Zhao for helpful discussions. Y.Z. thanks Professor Fangfu Ye for encouragement and support. The computations in this paper are carried out in the HPC computing cluster of ITP-CAS. H.J.Z. was supported by the National Basic Research Program of China (Grant No. 2013CB932804) and by the National Natural Science Foundation of China (Grants No. 11121403

and No. 11225526). S.M.Q. was partially supported by the Scientific Research Starting Foundation of Civil Aviation University of China (Grant No. 2015QD09S).

#### APPENDIX A: REPLICASYMMETRIC MEAN-FIELD THEORY UNDER AN ADDITIONAL ASSUMPTION

In this Appendix we analytically solve the RS mean-field theory for the ensemble of regular random (RR) graphs. Since every vertex in such a graph has the same number  $K$  of nearest neighbors and there is no structural correlations in the connectivity pattern, for analytic tractability we make an additional assumption here, namely the cavity probability distributions  $q_{i \rightarrow j}^{A_i}$  are identical for different pairs of neighboring vertices  $i$  and  $j$ . Then, according to the BP equation (8), we have  $q_{i \rightarrow j}^0 = 1 - a$  and  $q_{i \rightarrow j}^i = b$ , with the constants  $a$  and  $b$  satisfying

$$a = \frac{(1 - a + b)^{K-1} + (K - 1)a(1 - a + b)^{K-2}}{e^{-\beta} + (1 - a + b)^{K-1} + (K - 1)a(1 - a + b)^{K-2}}, \quad (\text{A1a})$$

$$b = \frac{(1 - a + b)^{K-1}}{e^{-\beta} + (1 - a + b)^{K-1} + (K - 1)a(1 - a + b)^{K-2}}. \quad (\text{A1b})$$

The energy density  $\rho$  is

$$\rho = \frac{e^{-\beta}}{e^{-\beta} + (1 - a + b)^K + Ka(1 - a + b)^{K-1}}, \quad (\text{A2})$$

and the free-energy density  $f$  is obtained from Eq. (10) as

$$f = -\frac{1}{\beta} \ln[e^{-\beta} + (1 - a + b)^K + Ka(1 - a + b)^{K-1}] + \frac{K}{2\beta} \ln[(1 - a)^2 + 2a(1 - a + b)]. \quad (\text{A3})$$

The minimum energy densities as obtained by this analytic theory are shown in the fourth column (RS-A) of Table I. Compared with the RS mean-field results in the third column obtained by population dynamics simulations (RS-P), we see that when  $K \geq 6$  the RS-A results are slightly lower than the RS-P results. We also observe that the RS-A results are less than the rigorous lower bounds in the second column of Table I [22], while the RS-P results are slightly higher than the rigorous lower bounds. The discrepancy between the RS-A and RS-P results must be due to the fact that the RS mean-field theory with all cavity probability distributions being identical is locally unstable at sufficiently high inverse temperature values [see Fig. 1(a)].

However, Fig. 1(a) also indicates that for  $K \rightarrow \infty$  the RS analytic theory will still be locally stable at  $\beta = \beta^*$  where the RS entropy density approaches zero. To work out the infinite- $K$  limit of the RS analytic theory, we notice that the parameters  $a$  and  $b$  of Eq. (A1) obey the following relationship

$$b = \frac{a}{1 + \frac{(K-1)a}{1-a+b}}. \quad (\text{A4})$$

At  $K \rightarrow \infty$  we have  $a \rightarrow 0$  and  $b \rightarrow 0$ , and then

$$b = \frac{a}{1 + (K-1)a}, \quad (\text{A5a})$$

$$\beta = \ln b - \ln(1-a) - (K-1)\ln(1-a+b). \quad (\text{A5b})$$

The free-energy density  $f$  at  $K \rightarrow \infty$  is expressed as

$$f = 1 + \frac{1}{\beta} \ln(1-a) + \frac{K}{2\beta} \ln(1-a^2+2ab). \quad (\text{A6})$$

The minimum energy density is determined by the condition of zero entropy density. Therefore we obtain

$$a\beta = -\ln(1-a) - \frac{K}{2} \ln(1-a^2+2ab). \quad (\text{A7})$$

By determining the values of  $a$ ,  $b$ , and  $\beta$  using Eqs. (A5) and (A7) at each value of degree  $K$ , we find that the minimum energy density  $\rho_0$  has the following asymptotic form:

$$\rho_0 = 1 - \frac{2 \ln K + c}{K} + o(K^{-1}) \quad (K \rightarrow \infty), \quad (\text{A8})$$

with parameter  $c \approx 2.05$ . This mean-field prediction agrees with the rigorous mathematical result of Haxell and coauthors [23], which states that  $c \leq (4 - 2 \ln 2) \approx 2.614$ .

## APPENDIX B: COMPUTING THERMODYNAMICAL QUANTITIES AT $y = \beta$

According to the 1RSB mean-field theory, the grand free energy density  $g$  for a given graph instance  $\mathcal{G}$  is

$$g = \frac{1}{N} \left( \sum_{i=1}^N g_i - \sum_{(i,j) \in \mathcal{G}} g_{ij} \right). \quad (\text{B1})$$

At  $y = \beta$ , the grand free energy contributions of a vertex  $i$  and an edge  $(i, j)$  are evaluated by the following simplified expressions:

$$g_i = -\frac{1}{\beta} \ln \left[ e^{-\beta} + \prod_{j \in \partial i} [\bar{q}_{j \rightarrow i}^0 + \bar{q}_{j \rightarrow i}^j] + \sum_{j \in \partial i} (1 - \bar{q}_{j \rightarrow i}^0) \prod_{k \in \partial i \setminus j} [\bar{q}_{k \rightarrow i}^0 + \bar{q}_{k \rightarrow i}^k] \right], \quad (\text{B2a})$$

$$g_{ij} = -\frac{1}{\beta} \ln [\bar{q}_{i \rightarrow j}^0 \bar{q}_{j \rightarrow i}^0 + (1 - \bar{q}_{i \rightarrow j}^0)(\bar{q}_{j \rightarrow i}^0 + \bar{q}_{j \rightarrow i}^j) + (1 - \bar{q}_{j \rightarrow i}^0)(\bar{q}_{i \rightarrow j}^0 + \bar{q}_{i \rightarrow j}^i)]. \quad (\text{B2b})$$

Similar to Eq. (B1), the mean free energy density  $\langle f \rangle$  of a macroscopic state is computed through

$$\langle f \rangle = \frac{1}{N} \left( \sum_{i=1}^N \langle f_i \rangle - \sum_{(i,j) \in \mathcal{G}} \langle f_{ij} \rangle \right). \quad (\text{B3})$$

The complexity  $\Sigma$  of the system at fixed values of  $\beta$  and  $y$  is simply  $\Sigma = y(\langle f \rangle - g)$ .

At  $y = \beta$ , the mean free energy contribution  $\langle f_i \rangle$  of a vertex  $i$  can be computed through

$$\langle f_i \rangle = \bar{q}_i^0 \langle f_i^0 \rangle + \bar{q}_i^i \langle f_i^i \rangle + \bar{q}_i^X \langle f_i^X \rangle. \quad (\text{B4})$$

In the above expression  $\bar{q}_i^0$ ,  $\bar{q}_i^i$ , and  $\bar{q}_i^X$  are the mean value of  $q_i^0$ ,  $q_i^i$ , and  $q_i^X$  over all the macroscopic states:

$$\bar{q}_i^0 = \frac{e^{-\beta}}{e^{-\beta} + \prod_{j \in \partial i} [\bar{q}_{j \rightarrow i}^0 + \bar{q}_{j \rightarrow i}^j] + \sum_{k \in \partial i} (1 - \bar{q}_{k \rightarrow i}^0) \prod_{j \in \partial i \setminus k} [\bar{q}_{j \rightarrow i}^0 + \bar{q}_{j \rightarrow i}^j]}, \quad (\text{B5a})$$

$$\bar{q}_i^i = \frac{\prod_{j \in \partial i} [\bar{q}_{j \rightarrow i}^0 + \bar{q}_{j \rightarrow i}^j]}{e^{-\beta} + \prod_{j \in \partial i} [\bar{q}_{j \rightarrow i}^0 + \bar{q}_{j \rightarrow i}^j] + \sum_{k \in \partial i} (1 - \bar{q}_{k \rightarrow i}^0) \prod_{j \in \partial i \setminus k} [\bar{q}_{j \rightarrow i}^0 + \bar{q}_{j \rightarrow i}^j]}, \quad (\text{B5b})$$

$$\bar{q}_i^X = \frac{\sum_{k \in \partial i} (1 - \bar{q}_{k \rightarrow i}^0) \prod_{j \in \partial i \setminus k} [\bar{q}_{j \rightarrow i}^0 + \bar{q}_{j \rightarrow i}^j]}{e^{-\beta} + \prod_{j \in \partial i} [\bar{q}_{j \rightarrow i}^0 + \bar{q}_{j \rightarrow i}^j] + \sum_{k \in \partial i} (1 - \bar{q}_{k \rightarrow i}^0) \prod_{j \in \partial i \setminus k} [\bar{q}_{j \rightarrow i}^0 + \bar{q}_{j \rightarrow i}^j]}, \quad (\text{B5c})$$

while the explicit expressions for  $\langle f_i^0 \rangle$ ,  $\langle f_i^i \rangle$ , and  $\langle f_i^X \rangle$  are

$$\langle f_i^0 \rangle = \prod_{j \in \partial i} \int \mathcal{D}q_{j \rightarrow i} [\bar{q}_{j \rightarrow i}^0 \mathcal{Q}_{j \rightarrow i}^0[q_{j \rightarrow i}] + \bar{q}_{j \rightarrow i}^j \mathcal{Q}_{j \rightarrow i}^j[q_{j \rightarrow i}] + \bar{q}_{j \rightarrow i}^X \mathcal{Q}_{j \rightarrow i}^X[q_{k \rightarrow i}]] f_i(\{q_{m \rightarrow i} : m \in \partial i\}), \quad (\text{B6a})$$

$$\langle f_i^i \rangle = \prod_{j \in \partial i} \int \mathcal{D}q_{j \rightarrow i} \left[ \frac{\bar{q}_{j \rightarrow i}^0}{\bar{q}_{j \rightarrow i}^0 + \bar{q}_{j \rightarrow i}^j} \mathcal{Q}_{j \rightarrow i}^0[q_{j \rightarrow i}] + \frac{\bar{q}_{j \rightarrow i}^j}{\bar{q}_{j \rightarrow i}^0 + \bar{q}_{j \rightarrow i}^j} \mathcal{Q}_{j \rightarrow i}^j[q_{j \rightarrow i}] \right] f_i(\{q_{m \rightarrow i} : m \in \partial i\}), \quad (\text{B6b})$$

$$\begin{aligned} \langle f_i^X \rangle &= \sum_{j \in \partial i} \omega_j \int \mathcal{D}q_{j \rightarrow i} \left[ \frac{\bar{q}_{j \rightarrow i}^j}{\bar{q}_{j \rightarrow i}^j + \bar{q}_{j \rightarrow i}^X} \mathcal{Q}_{j \rightarrow i}^j[q_{j \rightarrow i}] + \frac{\bar{q}_{j \rightarrow i}^X}{\bar{q}_{j \rightarrow i}^j + \bar{q}_{j \rightarrow i}^X} \mathcal{Q}_{j \rightarrow i}^X[q_{j \rightarrow i}] \right] \\ &\times \prod_{k \in \partial i \setminus j} \int \mathcal{D}q_{k \rightarrow i} \left[ \frac{\bar{q}_{k \rightarrow i}^0}{\bar{q}_{k \rightarrow i}^0 + \bar{q}_{k \rightarrow i}^k} \mathcal{Q}_{k \rightarrow i}^0[q_{k \rightarrow i}] + \frac{\bar{q}_{k \rightarrow i}^k}{\bar{q}_{k \rightarrow i}^0 + \bar{q}_{k \rightarrow i}^k} \mathcal{Q}_{k \rightarrow i}^k[q_{k \rightarrow i}] \right] f_i(\{q_{m \rightarrow i} : m \in \partial i\}), \quad (\text{B6c}) \end{aligned}$$

with

$$\omega_j = \frac{(1 - \bar{q}_{j \rightarrow i}^0) \prod_{k \in \partial i \setminus j} [\bar{q}_{k \rightarrow i}^0 + \bar{q}_{k \rightarrow i}^k]}{\sum_{l \in \partial i} (1 - \bar{q}_{l \rightarrow i}^0) \prod_{k \in \partial i \setminus l} [\bar{q}_{k \rightarrow i}^0 + \bar{q}_{k \rightarrow i}^k]}. \quad (\text{B7})$$

The mean free energy contribution  $\langle f_{ij} \rangle$  of an edge  $(i, j)$  can be computed through

$$\langle f_{ij} \rangle = \omega_{ij}^0 \langle f_{ij}^0 \rangle + \omega_{ij}^i \langle f_{ij}^i \rangle + \omega_{ij}^j \langle f_{ij}^j \rangle, \quad (\text{B8})$$

---

**Algorithm 1** IRSB population dynamics at  $y = \beta$

---

Construct a population of  $\mathcal{N}$  elements. The  $j$ -th element of this population a set of four cavity probability distributions  $\{A_j, B_j, C_j, D_j\}$  with the specific initial condition  $B_j = (1, 0, 0)$ ,  $C_j = (0, 1, 0)$ , and  $D_j = (0, 0, 1)$ .

**for**  $t = 1, 2, \dots, T_{\max}$  **do**

**for**  $r = 1, 2, \dots, \mathcal{N}$  **do**

    Generate a degree  $d$  according to the excess degree distribution  $Q(d)$ .

    Generate an integer set  $\partial i \setminus i' = \{j_1, j_2, \dots, j_{(d-1)}\}$  of size  $(d-1)$ , each element of which is sampled uniformly at random and with replacement from the set  $\{1, 2, \dots, \mathcal{N}\}$ , and then set the mean cavity probability distributions  $\bar{q}_{j_m \rightarrow i} = A_{j_m}$  for each  $j_m \in \partial i$ .

    Obtain a new mean cavity probability distribution  $A_{i \rightarrow i'}$  according to the BP equation:  $A_{i \rightarrow i'} = b(\{\bar{q}_{j_m \rightarrow i}\})$ .

**for**  $j_m \in \partial i \setminus i'$  **do**

      Set cavity probability distribution  $q_{j_m \rightarrow i} = B_{j_m}$  (with probability  $\bar{q}_{j_m \rightarrow i}^0$ ) or  $q_{j_m \rightarrow i} = C_{j_m}$  (with probability  $\bar{q}_{j_m \rightarrow i}^{j_m}$ ) or  $q_{j_m \rightarrow i} = D_{j_m}$  (with probability  $\bar{q}_{j_m \rightarrow i}^X$ ).

**end for**

    Obtain a new cavity probability distribution according to the BP equation:  $B_{i \rightarrow i'} = b(q_{j_m \rightarrow i})$ .

**for**  $j_m \in \partial i \setminus i'$  **do**

      Set cavity probability distribution  $q_{j_m \rightarrow i} = B_{j_m}$  (with probability  $\bar{q}_{j_m \rightarrow i}^0 / (\bar{q}_{j_m \rightarrow i}^0 + \bar{q}_{j_m \rightarrow i}^{j_m})$ ) or  $q_{j_m \rightarrow i} = C_{j_m}$  (with probability  $\bar{q}_{j_m \rightarrow i}^{j_m} / (\bar{q}_{j_m \rightarrow i}^0 + \bar{q}_{j_m \rightarrow i}^{j_m})$ ).

**end for**

    Obtain a new cavity probability distribution according to the BP equation:  $C_{i \rightarrow i'} = b(q_{j_m \rightarrow i})$ .

    Select one element  $j_m$  from set  $\partial i \setminus i'$  according to the probability  $\omega_{j_m \rightarrow i}$  of Eq. (39).

**for** each element  $j_{m'} \in \partial i \setminus i'$  **do**

**if**  $j_{m'}$  is equal to  $j_m$  **then**

        Set cavity probability distribution  $q_{j_{m'} \rightarrow i} = C_{j_{m'}}$  (with probability  $\bar{q}_{j_{m'} \rightarrow i}^{j_m} / (\bar{q}_{j_{m'} \rightarrow i}^{j_m} + \bar{q}_{j_{m'} \rightarrow i}^X)$ ) or  $q_{j_{m'} \rightarrow i} = D_{j_{m'}}$  (with probability  $\bar{q}_{j_{m'} \rightarrow i}^X / (\bar{q}_{j_{m'} \rightarrow i}^{j_m} + \bar{q}_{j_{m'} \rightarrow i}^X)$ ).

**else**

        Set cavity probability distribution  $q_{j_{m'} \rightarrow i} = B_{j_{m'}}$  (with probability  $\bar{q}_{j_{m'} \rightarrow i}^0 / (\bar{q}_{j_{m'} \rightarrow i}^0 + \bar{q}_{j_{m'} \rightarrow i}^{j_{m'}})$ ) or  $q_{j_{m'} \rightarrow i} = C_{j_{m'}}$  (with probability  $\bar{q}_{j_{m'} \rightarrow i}^{j_{m'}} / (\bar{q}_{j_{m'} \rightarrow i}^0 + \bar{q}_{j_{m'} \rightarrow i}^{j_{m'}})$ ).

**end if**

**end for**

    Obtain a new cavity probability distribution according to the BP equation:  $D_{i \rightarrow i'} = b(q_{j_m \rightarrow i})$ .

    Sample an index  $k$  uniformly at random from the set  $\{1, 2, \dots, \mathcal{N}\}$ , and then replace the  $k$ -th element of the population by the assembled element  $(A_{i \rightarrow i'}, B_{i \rightarrow i'}, C_{i \rightarrow i'}, D_{i \rightarrow i'})$ .

**end for**

**end for**

---

where

$$\omega_{ij}^0 = \frac{\bar{q}_{i \rightarrow j}^0 \bar{q}_{j \rightarrow i}^0}{\bar{q}_{i \rightarrow j}^0 \bar{q}_{j \rightarrow i}^0 + (1 - \bar{q}_{i \rightarrow j}^0)(\bar{q}_{j \rightarrow i}^0 + \bar{q}_{j \rightarrow i}^j) + (1 - \bar{q}_{j \rightarrow i}^0)(\bar{q}_{i \rightarrow j}^0 + \bar{q}_{i \rightarrow j}^j)}, \quad (\text{B9a})$$

$$\omega_{ij}^i = \frac{(1 - \bar{q}_{i \rightarrow j}^0)(\bar{q}_{j \rightarrow i}^0 + \bar{q}_{j \rightarrow i}^j)}{\bar{q}_{i \rightarrow j}^0 \bar{q}_{j \rightarrow i}^0 + (1 - \bar{q}_{i \rightarrow j}^0)(\bar{q}_{j \rightarrow i}^0 + \bar{q}_{j \rightarrow i}^j) + (1 - \bar{q}_{j \rightarrow i}^0)(\bar{q}_{i \rightarrow j}^0 + \bar{q}_{i \rightarrow j}^j)}, \quad (\text{B9b})$$

$$\omega_{ij}^j = \frac{(1 - \bar{q}_{j \rightarrow i}^0)(\bar{q}_{i \rightarrow j}^0 + \bar{q}_{i \rightarrow j}^j)}{\bar{q}_{i \rightarrow j}^0 \bar{q}_{j \rightarrow i}^0 + (1 - \bar{q}_{i \rightarrow j}^0)(\bar{q}_{j \rightarrow i}^0 + \bar{q}_{j \rightarrow i}^j) + (1 - \bar{q}_{j \rightarrow i}^0)(\bar{q}_{i \rightarrow j}^0 + \bar{q}_{i \rightarrow j}^j)}, \quad (\text{B9c})$$

and

$$\langle f_{ij}^0 \rangle = \int \mathcal{D}q_{j \rightarrow i} \mathcal{Q}_{j \rightarrow i}^0[q_{j \rightarrow i}] \int \mathcal{D}q_{i \rightarrow j} \mathcal{Q}_{i \rightarrow j}^0[q_{i \rightarrow j}] f_{ij}(q_{i \rightarrow j}, q_{j \rightarrow i}), \quad (\text{B10a})$$

$$\begin{aligned} \langle f_{ij}^i \rangle &= \int \mathcal{D}q_{i \rightarrow j} \left[ \frac{\bar{q}_{i \rightarrow j}^i}{\bar{q}_{i \rightarrow j}^i + \bar{q}_{i \rightarrow j}^X} \mathcal{Q}_{i \rightarrow j}^i[q_{i \rightarrow j}] + \frac{\bar{q}_{i \rightarrow j}^X}{\bar{q}_{i \rightarrow j}^i + \bar{q}_{i \rightarrow j}^X} \mathcal{Q}_{i \rightarrow j}^X[q_{i \rightarrow j}] \right] \\ &\times \int \mathcal{D}q_{j \rightarrow i} \left[ \frac{\bar{q}_{j \rightarrow i}^0}{\bar{q}_{j \rightarrow i}^0 + \bar{q}_{j \rightarrow i}^j} \mathcal{Q}_{j \rightarrow i}^0[q_{j \rightarrow i}] + \frac{\bar{q}_{j \rightarrow i}^j}{\bar{q}_{j \rightarrow i}^0 + \bar{q}_{j \rightarrow i}^j} \mathcal{Q}_{j \rightarrow i}^j[q_{j \rightarrow i}] \right] f_{ij}(q_{i \rightarrow j}, q_{j \rightarrow i}), \end{aligned} \quad (\text{B10b})$$

$$\begin{aligned} \langle f_{ij}^j \rangle &= \int \mathcal{D}q_{i \rightarrow j} \left[ \frac{\bar{q}_{i \rightarrow j}^0}{\bar{q}_{i \rightarrow j}^0 + \bar{q}_{i \rightarrow j}^i} \mathcal{Q}_{i \rightarrow j}^0[q_{i \rightarrow j}] + \frac{\bar{q}_{i \rightarrow j}^i}{\bar{q}_{i \rightarrow j}^0 + \bar{q}_{i \rightarrow j}^i} \mathcal{Q}_{i \rightarrow j}^i[q_{i \rightarrow j}] \right] \\ &\times \int \mathcal{D}q_{j \rightarrow i} \left[ \frac{\bar{q}_{j \rightarrow i}^j}{\bar{q}_{j \rightarrow i}^j + \bar{q}_{j \rightarrow i}^X} \mathcal{Q}_{j \rightarrow i}^j[q_{j \rightarrow i}] + \frac{\bar{q}_{j \rightarrow i}^X}{\bar{q}_{j \rightarrow i}^j + \bar{q}_{j \rightarrow i}^X} \mathcal{Q}_{j \rightarrow i}^X[q_{j \rightarrow i}] \right] f_{ij}(q_{i \rightarrow j}, q_{j \rightarrow i}). \end{aligned} \quad (\text{B10c})$$

### APPENDIX C: 1RSB POPULATION DYNAMICS SIMULATIONS AT $y = \beta$

To perform the 1RSB population dynamics simulation at  $y = \beta$  for the ER or RR graph ensemble, a population of  $\mathcal{N} \gg 1$  elements is first constructed, with the  $j$ th element of this population being a set of four cavity probability distributions:  $\{A_j, B_j, C_j, D_j\}$ . The cavity probability distribution  $A_j \equiv (A_j^0, A_j^j, A_j^X)$  is the mean cavity probability distribution  $\bar{q}_{j \rightarrow i} \equiv (\bar{q}_{j \rightarrow i}^0, \bar{q}_{j \rightarrow i}^j, \bar{q}_{j \rightarrow i}^X)$  on an edge  $(i, j)$ ,  $B_j \equiv (B_j^0, B_j^j, B_j^X)$  is a sampled cavity probability distribution from the probability functional  $\mathcal{Q}_{j \rightarrow i}^0[q_{j \rightarrow i}]$ ,  $C_j \equiv (C_j^0, C_j^j, C_j^X)$  is a sampled cavity probability distribution from the probability functional  $\mathcal{Q}_{j \rightarrow i}^j[q_{j \rightarrow i}]$ , and  $D_j \equiv (D_j^0, D_j^j, D_j^X)$  is a sampled cavity probability distribution from the probability functional  $\mathcal{Q}_{j \rightarrow i}^X[q_{j \rightarrow i}]$ .

The elements of the population are updated according to Eq. (38), see Algorithm 1 for more implementation details. In our actual simulations we set the population size as  $\mathcal{N} = 128\,000$  and total simulation steps as  $T_{\max} = 144\,000$ . The first 16 000 simulation steps are used to drive the population to a steady state, and the remaining 128 000 steps are used for population further updating and for computing the grand free energy density  $g$ , the mean free energy density  $\langle f \rangle$ , and the complexity  $\Sigma$ . Figure 2 shows some of the simulation results for the RR graph ensemble. To evaluate and minimize the errors of our computation, each data point in Fig. 2 is the mean value of 16 independent running of the simulation algorithm with different random number seeds, and the error bar of each data point is the standard error of the mean.

### APPENDIX D: SOLVING THE INFINITE- $\beta$ 1RSB MEAN-FIELD THEORY

Here we first describe the 1RSB population dynamics (1RSB-P) method to solve the iterative equation (45) at the graph ensemble level. First a population of size  $\mathcal{N}$  is constructed, with the  $m$ th member of which being itself a subpopulation (denoted as  $\mathcal{Q}_m[\chi]$ ) of  $\mathcal{M}$  infinite- $\beta$  cavity messages of the form  $\chi \equiv (\gamma_{i \rightarrow j}, \rho_{i \rightarrow j}, \eta_{i \rightarrow j})$ . The subpopulation  $\mathcal{Q}_m[\chi]$  represents the cavity probability functional  $\mathcal{Q}_{i \rightarrow j}[\chi_{i \rightarrow j}]$  of a randomly chosen edge  $(i, j)$  in the graph ensemble.

In our simulations for the RR graph ensemble we take  $\mathcal{N} = 10^4$  and  $\mathcal{M} = 10^4$  (we have checked that the simulation results are quite insensitive to the precise values of  $\mathcal{N}$  and  $\mathcal{M}$ ). The 1RSB-P steps of updating the  $\mathcal{N}$  elements of the population are described in Algorithm 2. The total number  $T_{\max}$  of simulation steps is set to be  $T_{\max} \approx 10^4$ .

We follow the method used in Ref. [28] for updating a single subpopulation  $\mathcal{Q}_m[\chi]$ , see Algorithm 3. In this reweighted sampling method, we first generate  $N_p \times \mathcal{M}$  cavity messages  $\chi^{(s)} \equiv (\gamma^{(s)}, \rho^{(s)}, \eta^{(s)})$  ( $s = 1, 2, \dots$ ) and assign each of these messages a weight  $w^{(s)} = e^{-y(1-\gamma^{(s)})}$ . Then we sample  $\mathcal{M}$  elements from these cavity messages (with replacement) according to their assigned weights. The integer parameter  $N_p$  control the level of sample abundance. A larger value of  $N_p$  will lead to more precise numerical results but the computational cost also be proportional to  $N_p$ . In our simulations we typically let  $1 \leq N_p \leq 10$  (we allow  $N_p$  to increase slightly with the parameter  $y$  of the 1RSB population dynamics).

---

**Algorithm 2** The infinite- $\beta$  1RSB population dynamics (1RSB-P) simulation process

---

Initial the population with  $\mathcal{N}$  subpopulations, each subpopulation containing  $\mathcal{M}$  elements of the form  $\chi = (\gamma_{i \rightarrow j}, \rho_{i \rightarrow j}, \eta_{i \rightarrow j})$ .

```

for  $t = 1, 2, \dots, T_{\max}$ 
  for  $r = 1, 2, \dots, \mathcal{N}$ 
    Generate a degree  $d$  according the excess degree distribution  $Q(d)$ .
    Generate an integer set  $\partial i \setminus i' = \{j_1, j_2, \dots, j_{(d-1)}\}$  of size  $(d-1)$  uniformly at random and with replacement from the index set  $\{1, 2, \dots, \mathcal{N}\}$ .
    for  $s = 1, 2, \dots, N_p \times \mathcal{M}$  do
      for  $j \in \partial i \setminus i'$  do
        Sample an element  $\chi_{j \rightarrow i}$  uniformly at random from the subpopulation  $Q_j[\chi]$ .
      end for
      Generate a new cavity message according to the SP(y) equation:  $\chi_{i \rightarrow i'}^{(s)} \equiv (\gamma_{i \rightarrow i'}^{(s)}, \rho_{i \rightarrow i'}^{(s)}, \eta_{i \rightarrow i'}^{(s)}) = b_{\infty}(\{\chi_{j \rightarrow i}\})$ ; and assign a weight  $W^{(s)} = \exp[-y(1 - \gamma_{i \rightarrow i'}^{(s)})]$  to this message.
    end for
    Replace the  $r$ th subpopulation of the population by the new subpopulation  $Q_r[\chi] = \text{REWEIGHT}(\{\chi_{i \rightarrow i'}^{(s)}, W^{(s)}\})$ .
  end for
end for

```

---

In the remaining part of this appendix we consider the integer-field approximation of the infinite- $\beta$  1RSB mean-field theory. Under the integer-field restriction, then the cavity quantities  $\gamma_{i \rightarrow j} \in \{0, 1\}$ ,  $\rho_{i \rightarrow j} \in \{0, 1\}$ , and  $\eta_{i \rightarrow j} \in \{-1, 0, 1\}$ . Because of the iterative equation (43), the cavity message  $\chi_{i \rightarrow j} \equiv \{\gamma_{i \rightarrow j}, \rho_{i \rightarrow j}, \eta_{i \rightarrow j}\}$  will be one of the following three possible types:

$$\chi_{001} = \{0, 0, 1\}, \chi_{100} = \{1, 0, 0\}, \chi_{11\bar{1}} = \{1, 1, -1\}. \quad (\text{D1})$$

---

**Algorithm 3** REWEIGHT ( $\{\chi^{(s)}, W^{(s)}\}$ )

---

```

for  $s = 1, 2, \dots, N_p \mathcal{M}$ 
  Set  $P_s \equiv W^{(s)} / \sum_{r=1}^{N_p \mathcal{M}} W^{(r)}$ .
end for
for  $s = 1, 2, \dots, \mathcal{M}$  do
  Generate  $r \in \{1, 2, \dots, N_p \mathcal{M}\}$  with probability  $P_r$ .
  Set  $\chi_{\text{new}}^{(s)} = \chi^{(r)}$ .
end for
return  $\{\chi_{\text{new}}^{(1)}, \chi_{\text{new}}^{(2)}, \dots, \chi_{\text{new}}^{(\mathcal{M})}\}$ .

```

---

Because of this nice property, the 1RSB probability functional  $Q_{i \rightarrow j}[\chi_{i \rightarrow j}]$  can be parameterized by three non-negative values  $m_{i \rightarrow j}^{001}$ ,  $m_{i \rightarrow j}^{100}$ , and  $m_{i \rightarrow j}^{11\bar{1}}$  which sum up to unity. The quantity  $m_{i \rightarrow j}^{001}$  is just the probability that the cavity message  $\chi_{i \rightarrow j}$  is of type  $\chi_{001}$  among all the macroscopic states. The other two parameters  $m_{i \rightarrow j}^{100}$  and  $m_{i \rightarrow j}^{11\bar{1}}$  can be similarly interpreted. Based on the SP(y) equation (43), we can get a set of self-consistent equations for these parameters. For the RR graph ensemble, if we in addition assume that  $m_{i \rightarrow j}^{001} = m_1$ ,  $m_{i \rightarrow j}^{100} = m_2$  and  $m_{i \rightarrow j}^{11\bar{1}} = m_3$ , then the three constants  $m_1, m_2, m_3$  are self-consistently determined through

$$m_1 = \frac{e^{-y}(1 - (1 - m_3)^{K-1} - (K-1)(1 - m_3)^{K-2}m_3)}{e^{-y} + (1 - e^{-y})[(1 - m_3)^{K-1} + (K-1)(1 - m_3)^{K-2}m_3]}, \quad (\text{D2a})$$

$$m_2 = \frac{(1 - m_3)^{K-1}}{e^{-y} + (1 - e^{-y})[(1 - m_3)^{K-1} + (K-1)(1 - m_3)^{K-2}m_3]}, \quad (\text{D2b})$$

$$m_3 = \frac{(K-1)(1 - m_3)^{K-2}m_3}{e^{-y} + (1 - e^{-y})[(1 - m_3)^{K-1} + (K-1)(1 - m_3)^{K-2}m_3]}. \quad (\text{D2c})$$

---

[1] P. Festa, P. M. Pardalos, and M. G. C. Resende, Feedback set problems, in *Handbook of Combinatorial Optimization*, edited by D.-Z. Du and P. M. Pardalos (Springer, Berlin, 1999), pp. 209–258.

[2] M. Garey and D. S. Johnson, *Computers and Intractability: A Guide to the Theory of NP-Completeness* (Freeman, San Francisco, 1979).

[3] D. Zöbel, The deadlock problem: a classifying bibliography, *SIGOPS Oper. Syst. Rev.* **17**, 6 (1983).

[4] B. Fiedler, A. Mochizuki, G. Kurosawa, and D. Saito, Dynamics and control at feedback vertex sets I: Informative and determining nodes in regulatory networks, *J. Dynam. Differ. Eq.* **25**, 563 (2013).

[5] A. Mochizuki, B. Fiedler, G. Kurosawa, and D. Saito, Dynamics and control at feedback vertex sets II: A faithful monitor to determine the diversity of molecular activities in regulatory networks, *J. Theor. Biol.* **335**, 130 (2013).

[6] A. Guggiola and G. Semerjian, Minimal contagious sets in random regular graphs, *J. Stat. Phys.* **158**, 300 (2015).

[7] S. Mugisha and H.-J. Zhou, Identifying optimal targets of network attack by belief propagation, *Phys. Rev. E* **94**, 012305 (2016).

[8] A. Braunstein, L. Dall’Asta, G. Semerjian, and L. Zdeborová, Network dismantling, [arXiv:1603.08883](https://arxiv.org/abs/1603.08883) (2016).

[9] R. M. Karp, Reducibility among combinatorial problems, in *Complexity of Computer Computations*, edited by E. Miller, J. W. Thatcher, and J. D. Bohlinger (Plenum Press, New York, 1972), pp. 85–103.

[10] D. Li and Y. Liu, A polynomial algorithm for finding the minimum feedback vertex set of a 3-regular simple graph, *Acta Math. Sci.* **19**, 375 (1999).

[11] Y. D. Liang, On the feedback vertex set problem in permutation graphs, *Inf. Proc. Lett.* **52**, 123 (1994).

[12] Y. D. Liang and M.-S. Chang, Minimum feedback vertex sets in cocomparability graphs and convex bipartite graphs, *Acta Inform.* **34**, 337 (1997).

[13] F. V. Fomin, S. Gaspers, A. V. Pyatkin, and I. Razgon, On the minimum feedback vertex set problem: Exact and enumeration algorithms, *Algorithmica* **52**, 293 (2008).

- [14] V. Bafna, P. Berman, and T. Fujito, A 2-approximation algorithm for the undirected feedback vertex set problem, *SIAM J. Discrete Math.* **12**, 289 (1999).
- [15] S.-M. Qin and H.-J. Zhou, Solving the undirected feedback vertex set problem by local search, *Eur. Phys. J. B* **87**, 273 (2014).
- [16] H.-J. Zhou, Spin glass approach to the feedback vertex set problem, *Eur. Phys. J. B* **86**, 455 (2013).
- [17] R. Monasson, Structural Glass Transition and the Entropy of the Metastable States, *Phys. Rev. Lett.* **75**, 2847 (1995).
- [18] M. Mézard and G. Parisi, The Bethe lattice spin glass revisited, *Eur. Phys. J. B* **20**, 217 (2001).
- [19] M. Mézard and A. Montanari, *Information, Physics, and Computation* (Oxford University Press, New York, 2009).
- [20] B. Bollobás, *Random Graphs*, 2nd ed. (Cambridge University Press, Cambridge, UK, 2001).
- [21] C. Hoppen and N. Wormald, Induced forests in regular graphs with large girth, *Combinat. Prob. Comput.* **17**, 389 (2008).
- [22] S. Bau, N. C. Wormald, and S. Zhou, Decycling numbers of random regular graphs, *Random Struct. Alg.* **21**, 397 (2002).
- [23] P. Haxell, O. Pikhurko, and A. Thomason, Maximum acyclic and fragmented sets in regular graphs, *J. Graph Theor.* **57**, 149 (2008).
- [24] F. Altarelli, A. Braunstein, L. Dall'Asta, and R. Zecchina, Optimizing spread dynamics on graphs by message passing, *J. Stat. Mech.: Theor. Exp.* (2013) P09011.
- [25] A. Montanari, G. Parisi, and F. Ricci-Tersenghi, Instability of one-step replica-symmetry-broken phase in satisfiability problems, *J. Phys. A: Math. Gen.* **37**, 2073 (2004).
- [26] A. Montanari and F. Ricci-Tersenghi, On the nature of the low-temperature phase in discontinuous mean-field spin glasses, *Eur. Phys. J. B* **33**, 339 (2003).
- [27] L. Zdeborová and M. Mézard, The number of matchings in random graphs, *J. Stat. Mech.: Theor. Exp.* (2006) P05003.
- [28] L. Zdeborová, Statistical physics of hard optimization problems, *Acta Phys. Slov.* **59**, 169 (2009).
- [29] P. Zhang, Y. Zeng, and H.-J. Zhou, Stability analysis on the finite-temperature replica-symmetric and first-step replica-symmetry-broken cavity solutions of the random vertex cover problem, *Phys. Rev. E* **80**, 021122 (2009).
- [30] T. R. Kirkpatrick and D. Thirumalai,  $p$ -spin-interaction spin-glass models: Connections with the structural glass problem, *Phys. Rev. B* **36**, 5388 (1987).
- [31] M. Mézard and R. Zecchina, Random  $K$ -satisfiability problem: From an analytic solution to an efficient algorithm, *Phys. Rev. E* **66**, 056126 (2002).
- [32] M. Mézard and A. Montanari, Reconstruction on trees and spin glass transition, *J. Stat. Phys.* **124**, 1317 (2006).
- [33] F. Krzakala, A. Montanari, F. Ricci-Tersenghi, G. Semerjian, and L. Zdeborová, Gibbs states and the set of solutions of random constraint satisfaction problems, *Proc. Natl. Acad. Sci. USA* **104**, 10318 (2007).
- [34] A. Montanari, F. Ricci-Tersenghi, and G. Semerjian, Clusters of solutions and replica symmetry breaking in random  $k$ -satisfiability, *J. Stat. Mech.: Theor. Exp.* (2008) P04004.
- [35] A. Braunstein, M. Mézard, and R. Zecchina, Survey propagation: An algorithm for satisfiability, *Random Struct. Alg.* **27**, 201 (2005).
- [36] A. Braunstein and R. Zecchina, Survey propagation as local equilibrium equations, *J. Stat. Mech.: Theor. Exp.* (2004) P06007.
- [37] H.-J. Zhou,  $T \rightarrow 0$  mean-field population dynamics approach for the random 3-satisfiability problem, *Phys. Rev. E* **77**, 066102 (2008).
- [38] F. Krzakala and L. Zdeborová, Potts glass on random graphs, *Europhys. Lett.* **81**, 57005 (2008).
- [39] H.-J. Zhou, Vertex cover problem studied by cavity method: Analytics and population dynamics, *Eur. Phys. J. B* **32**, 265 (2003).
- [40] O. Rivoire, G. Biroli, O. C. Martin, and M. Mézard, Glass models on bethe lattices, *Eur. Phys. J. B* **37**, 55 (2004).
- [41] S. Franz, M. Leone, F. Ricci-Tersenghi, and R. Zecchina, Exact Solutions for Diluted Spin Glasses and Optimization Problems, *Phys. Rev. Lett.* **87**, 127209 (2001).
- [42] S. Franz, M. Mézard, R. Ricci-Tersenghi, M. Weigt, and R. Zecchina, A ferromagnet with a glass transition, *Europhys. Lett.* **55**, 465 (2001).
- [43] A. Coja-Oghlan and C. Efthymiou, On independent sets in random graphs, *Rand. Struct. Algor.* **47**, 436 (2015).
- [44] J. Barbier, F. Krzakala, L. Zdeborová, and P. Zhang, The hardcore model on random graphs revisited, *J. Phys.: Conf. Series* **473**, 012021 (2013).
- [45] R. Monasson and R. Zecchina, Statistical mechanics of the random  $K$ -satisfiability model, *Phys. Rev. E* **56**, 1357 (1997).